AD_____

Award Number: **W81XWH-08-1-0318**

TITLE: **LL-37 Recruits Immunosuppressive Regulatory T Cells to Ovarian Tumors**

PRINCIPAL INVESTIGATOR: **Aline B. Betancourt, Ph.D. (Scandurro formerly)**

CONTRACTING ORGANIZATION: **Tulane University**
New Orleans, LA 70112

REPORT DATE: **November 2009**

TYPE OF REPORT: **Final**

PREPARED FOR: U.S. Army Medical Research and Materiel Command
Fort Detrick, Maryland 21702-5012

DISTRIBUTION STATEMENT:

√ Approved for public release; distribution unlimited

REPORT DOCUMENTATION PAGE

Form Approved
OMB No. 0704-0188

1. REPORT DATE	2. REPORT TYPE	3. DATES COVERED
01-11-2009	Final	04-15-08- To 10-14-09

4. TITLE AND SUBTITLE
LL-37 Recruits Immunosuppressive Regulatory T Cells to Ovarian Tumors

5a. CONTRACT NUMBER
W81XWH-08-1-0318

5b. GRANT NUMBER

5c. PROGRAM ELEMENT NUMBER

6. AUTHOR(S)
Aline M. Betancourt, PhD (formerly Aline B. Scandurro, PhD)

Email: alibscan@tulane.edu

5d. PROJECT NUMBER

5e. TASK NUMBER

5f. WORK UNIT NUMBER

7. PERFORMING ORGANIZATION NAME(S) AND ADDRESS(ES)

Tulane University
New Orleans, LA 70112

8. PERFORMING ORGANIZATION REPORT NUMBER

9. SPONSORING / MONITORING AGENCY NAME(S) AND ADDRESS(ES)
U.S. Army Medical Research and Materiel Command
Fort Detrick, Maryland 21702-5012

10. SPONSOR/MONITOR'S ACRONYM(S)

11. SPONSOR/MONITOR'S REPORT NUMBER(S)

12. DISTRIBUTION / AVAILABILITY STATEMENT
Approved for Public Release; Distribution Unlimited

13. SUPPLEMENTARY NOTES

14. ABSTRACT

Histological examination of ovarian, breast, and lung tumors has shown that the pro-inflammatory peptide, LL-37, is abnormally elevated. LL-37 was originally identified as one of the host defense peptides that is released during infections to attack microorganisms. Recent studies established other functions for LLin immune responses, tissue injury and inflammation. LL-37 is highly elevated at sites of inflammation and wound healing where it is a mitogen and pro-angiogenic factor. LL-37 also acts as a potent chemoattractant for various immune cells. In contrast to LL-37's established functions in host defense and tissue damage, its role in the tumor microenvironment and the advantage given to tumor cells by its and its receptor's expression is not entirely clear. Our studies indicate that LL-37's functions are multifaceted in solid tumors, where evidence exists for its role as a mitogen, pro-angiogenic factor, and leukocyte chemoattractant. Specifically we were first to show that: • LL-37 levels are highly elevated in ovarian cancer when compared to normal ovarian tissue. • LL-37 specifically affects the growth and spread of ovarian cancer cells. • LL37 in the ovarian cancer tumors specifically recruits mesenchymal stem cells (MSC). • MSCs recruited to the cancer microenvironment promote tumor growth and spread.

15. SUBJECT TERMS
pro-inflammatory antimicrobial peptides, cathelicidins, LL-37, ovarian cancer, mesenchymal stem cells, immune modulation, tumor microenvironment

16. SECURITY CLASSIFICATION OF:			17. LIMITATION OF ABSTRACT	18. NUMBER OF PAGES	19a. NAME OF RESPONSIBLE PERSON
a. REPORT	b. ABSTRACT	c. THIS PAGE			USAMRMC
U	U	U	UU	42	19b. TELEPHONE NUMBER *(include area code)*

Table of Contents

Page

INTRODUCTION:

Tumors depend on a permissive and supportive microenvironment for their growth and spread. Emerging evidence suggests that both resident and recruited bone marrow-derived cells play a critical and supportive role in creating a favorable immunosuppressive tumor microenvironment. Clinical observations support this notion since an increased prevalence of recruited leukocytes in tumors is correlated with a poor prognosis for the affected patient. By contrast, therapies that eradicate certain immune cells from the tumor microenvironment lead to longer remission periods for the treated patient. Among the recruited cells, multipotent mesenchymal stromal cells (MSCs) formerly known as mesenchymal stem cells are also known to proceed from the bone marrow to tumors, and once there to reside within tumor stromal microenvironments. MSCs are known to be highly immunosuppressive and exhibit many of the same mechanisms ascribed to a pro-tumor immune microenvironment. For instance, MSCs inhibit dendritic cell maturation, B and T cell proliferation and differentiation, as well as attenuate natural killer cell killing, and also support suppressive T regulatory cells (Tregs). This proposal builds on our recent reports that established that elevated levels of the human pro-inflammatory antimicrobial peptide LL-37 secreted from ovarian cancer cells recruit MSCs to the growing tumor. Our work suggested that MSCs resident in this tumor microenvironment increased ovarian cancer growth and spread. Our ***hypothesis*** is that ovarian tumor-derived LL-37 contributes to tumor-induced immunosuppression through recruitment and modulation of regulatory T cells (Tregs). Our ***aims*** to test this hypothesis were to: a) characterize the effects of LL-37 on regulatory T cell chemotaxis and function *in vitro* and; b) determine if tumor-derived LL-37 recruits regulatory T cells to the ovarian tumor microenvironment. The potential impact of altering the balance from permissive and supportive tumor microenvironments to one of tumor eradication in new treatment regimens is only beginning to be recognized. It is expected that the information gained from this study will potentially identify new therapeutic targets, provide new markers for earlier diagnoses of ovarian cancer and may establish new parameters that better predict the course of the disease.

BODY:

We have included the study as it was described in our Statement of Work and following each section presented what we have accomplished based on the proposed work.

Task 1. To characterize the effects of LL-37 on regulatory T cell (Tregs) chemotaxis and function *in vitro* (Months 1-12):

a. *Develop optimal assays to isolate Tregs from human buffy coats.*
b. *Chemotaxis assays will be performed with established Tregs pools (a.) as follows: recombinant LL-37 peptide will be used to stimulate Tregs chemotaxis in a modified Boyden chamber and will be compared with CCL22, an established chemotactic factor for Tregs.*
c. *Proliferation assays will be performed to measure the effect of LL-37 on Tregs.*
d. *Analyze the LL-37-treated Tregs by flow cytometry or ELISA for changes in CD25, FOXP3, CTLA-4, CCR4, TGF-β, and IL-10 marker expression.*

As a result of initial indications that ovarian cancer cells secrete LL-37 that then recruits mesenchymal stem cells (MSCs) that have the ability to then recruit and/or convert T regulatory cells (Tregs) we undertook experiments that explored this aspect first in our studies. Note, all figures and tables are located under the Supporting Data section.

Investigations carried out in our laboratory have centered on understanding the mechanisms by which environmental factors, especially those surrounding tumor microenvironments, affect the recruitment, migration and pro-angiogenesis potential of human adult bone marrow-derived multipotent stromal cells (MSCs). These cells are obtained as such from the Tulane Center for Gene Therapy, an NCI-funded facility that provides these cells to investigators. These cells are also obtained from commercial sources (Lonza Corp., East Rutheford, NJ). Enhanced levels of LL-37 in the ovarian tumors were also found to correlate with increased leukocyte infiltration. Further, these studies showed that MSCs are recruited to the ovarian tumors via engagement of their LL-37 receptor formyl receptor-like 1 (FPRL-1). Additionally, our work suggested that MSCs resident in the tumor microenvironment increased ovarian cancer growth and served to organize the fibrovascular networks within the tumor stroma (Coffelt, Waterman et al. 2008; Tomchuck, Zwezdaryk et al. 2008; Coffelt, Marini et al. 2009). Putting all these observations together we explore here the possibility that the MSCs recruited to the ovarian tumor microenvironment are not just acting to promote angiogenesis but also to set-up an immunosuppressive host response that favors the tumor's growth and spread by supporting Tregs recruitment.

The pro-inflammatory peptide, LL-37, promotes ovarian tumor progression through recruitment of multipotent mesenchymal stromal cells.

Given the similar expression pattern of LL-37 in tumors, damaged tissue, and inflammation, where MSCs are prominent, as well as the ability of the peptide to stimulate chemotaxis of various cell types, we hypothesized that ovarian tumor-derived LL-37 recruits MSCs to the tumor microenvironment to support cancer progression. Since LL-37 has been shown to activate migration through the FPRL1 receptor in various cell types, several donor pools of MSC were examined for expression of FPRL1 (Yang, Chen et al. 2000; Tjabringa, Ninaber et al. 2006). Flow cytometry analyses confirmed the expression of FPRL1 on all MSC donor pools corroborating results from other laboratories (**Figure 1A**) (Viswanathan, Painter et al. 2007).

We extended our previous findings to determine the optimal dosage of the peptide using *in vitro* chemotaxis assays. LL-37 induced the migration of MSC in a dose-dependent manner

and the peptide performed as well as epidermal growth factor (EGF), an established chemotactic factor for these cells (Nakamizo, Marini et al. 2005). MSC were pretreated with pertussis toxin (Ptx), a $G_{\alpha i}$ inhibitor, before activation with LL-37 or EGF to prevent FPRL1 signaling. Ptx treatment followed by LL-37 stimulation resulted in a significant inhibition of MSC migration, whereas no significant difference was observed between EGF-stimulated, Ptx-treated cells and EGF-stimulated cells alone. LL-37 and EGF were also preincubated with a neutralizing LL-37 antibody and, as expected, the neutralizing antibody (αLL-37) abolished LL-37's chemotactic effects on MSC, but had no effect on EGF-stimulated cells. No decrease in MSC migration was observed in wells with a control IgG antibody (data not shown).

MSC invasion through Matrigel-coated inserts was also significantly enhanced by LL-37 stimulation (**Figure 1D**). Pretreatment of MSC with Ptx significantly attenuated LL-37's ability to promote invasion (**Figure 1E**). EGF-stimulated cells were slightly affected by Ptx, but this was not significant. The anti-LL-37 antibody (αLL-37) significantly blocked LL-37 from binding to MSC surface receptors, since MSC in this experimental group did not invade as effectively (**Figure 1E**). By contrast, the anti-LL-37 antibody did not affect EGF stimulation of MSC invasion. An IgG control antibody did not interfere with the ability of LL-37 or EGF to induce MSC invasion (data not shown). Taken together, these data suggest that LL-37 induces MSC trafficking through a $G_{\alpha i}$-coupled receptor, such as FPRL1.

As further validation of FPRL1 involvement in LL-37-mediated responses, MSC were assessed for activation of signaling molecules downstream of this receptor. Western blot analysis of MSC lysates showed that ERK-1 and -2 are robustly phosphorylated beginning 10 minutes after LL-37 treatment and maintained over 60 minutes (**Figure 1F, G**). However, MSC pretreated with Ptx before stimulation by LL-37 reduced ERK-1/2 activation, providing further evidence in support of notion that LL-37 stimulates MSC through FPRL1.

FPRL1 is expressed on ovarian cancer cells and LL-37 does not signal through a G protein-coupled receptor, such as FPRL1, to stimulate ovarian cancer cell proliferation.

A panel of seven cell lines was examined by flow cytometry for expression of FPRL1. The ovarian cancer cell lines expressed FPRL1 to varying degrees and Hs832.Tc – a fibroblastic cell line derived from a benign ovarian cyst – expressed the lowest measured levels of FPRL1 (**Figure 2**). We previously reported that LL-37 induces ovarian cancer cell proliferation (Coffelt, Waterman et al. 2008). To determine if LL-37 signals through FPRL1 to mediate this effect, the same ovarian cancer cell lines used in our prior study were pretreated with pertussis toxin (Ptx) before exposure to the LL-37 peptide. Ptx treatment reduced the proliferation rate of LL-37-treated HEY, OV-90, and SK-OV-3 cells after 48 hours; although, this effect was not statistically significant (**Figure 3**). These results indicate that LL-37 does not use FPRL1 (or any other GPCR) to stimulate ovarian cancer cell growth.

LL-37 mediates ovarian cancer cell migration and invasion through FPRL1

Previously, we also reported that LL-37 enhances the metastatic potential of ovarian cancer cells (Coffelt, Waterman et al. 2008). Since FPRL1 is involved in LL-37-mediated chemotaxis of some lymphoid and myeloid subsets, we hypothesized that LL-37 utilizes this receptor to initiate ovarian cancer cell migration and invasion (Yang, Chen et al. 2000; Tjabringa, Ninaber et al. 2006). To address this question, preliminary experiments were conducted using SK-OV-3 cells in a modified Boyden chamber chemotaxis assay. SK-OV-3 cells were pretreated with or without Ptx, loaded into the chamber, and stimulated with LL-37 or EGF. In this assay, Ptx abrogated the migratory effects of LL-37 on SK-OV-3 cells, but had no significant affect on EGF-stimulated migration (**Figure 4A**), suggesting that LL-37 may signal through FPRL1 whereas EGF does not use a GPCR. We then established FPRL1 knockdown cells by transduction of SK-OV-3 cells with lentiviruses containing FPRL1-specific shRNA constructs (FPRL1 KD-1 through 5). Another shRNA construct that does not recognize a

specific mRNA target (called non-target or NT) was used as control. *Fprl1* gene expression was measured using quantitative real-time PCR (qPCR) and it was observed that *fprl1* expression was significantly diminished in SK-OV-3/FPRL1 KD-1, -2, -3, -4 cells (**Figure 4B**). SK-OV-3/FPRL1 KD-2 cells were chosen for use in subsequent experiments, as the level of *fprl1* mRNA transcript was lowest in these cells. SK-OV-3 cells seeded onto Matrigel-coated inserts were then stimulated with LL-37 or EGF in an *in vitro* metastasis assay. Like the migration assay results, LL-37-induced SK-OV-3 cell invasion through Matrigel was attenuated by Ptx, whereas EGF-stimulated invasion was unaffected by the inhibitor (**Figure 4C, left panel**). SK-OV-3 cells transfected with control shRNA vectors (NT) responded to LL-37 and EGF stimulation in a similar manner as untransfected cells (**Figure 4C, right panel**). Unexpectedly, SK-OV-3/FPRL1 KD-2 cells were significantly more invasive than the NT cells. EGF exposure significantly augmented their invasive behavior, but LL-37 stimulation failed to significantly enhance SK-OV-3/FPRL1 KD-2 cell invasion when compared to untreated, knockdown cells. Taken together, these data suggest that LL-37 signals through FPRL1 to increase the metastaic potential of ovarian cancer cells.

*Activation of MAPK signaling pathways by LL-37 does not occur through FPRL1***.**

To better define the signaling pathways that are activated by LL-37, several of the established FPRL1- and EGFR-associated signaling cascades were studied (Koczulla, von Degenfeld et al. 2003; Tjabringa, Aarbiou et al. 2003; Bowdish, Davidson et al. 2004; Heilborn, Nilsson et al. 2005; Tokumaru, Sayama et al. 2005; Carretero, Escamez et al. 2008; von Haussen, Koczulla et al. 2008). Western blot analysis of LL-37-treated SK-OV-3 cell lysates showed the robust phosphorylation of ERK1/2 and a slight activation of STAT3 after the indicated time points (**Figure 5A**). By contrast, AKT activation was constitutive for the time points measured. Similar results were observed in LL-37-treated OVCAR-3 cells (data not shown). SK-OV-3 cells were pretreated with Ptx before LL-37 stimulation, but ERK1/2 phosphorylation was maintained despite inhibition of GPCR signaling (**Figure 5B**). These observations were confirmed using SK-OV-3/FPRL1 KD-2 cells, indicating that LL-37-induced MAPK signaling does not occur through FPRL1 (or another GPCR).

Inhibition of FPRL1 negatively affects LL-37-induced nuclear accumulation and activity of multiple transcription factors.

Nuclear protein extracts isolated from LL-37-treated ovarian cancer cells were then analyzed using a Luminex-based assay, as a quantitative measurement of LL-37-activated signaling pathways at the transcription factor level. This method allowed us to measure not only nuclear accumulation of the transcription factors, but also activation, since fluorescence intensity is based on DNA binding activity to specific oligonucleotide probes. LL-37 induced a number of transcription factors in SK-OV-3 and OVCAR-3 cells; however, only those transcription factors that were increased more than four fold were analyzed for statistical significance. The transcription factors that were significantly increased in both cell lines when compared with untreated cells included CREB, ELK1, estrogen receptor (ER), FAST1, GATA, glucocorticoid receptor/progesterone receptor (GR/PR), PPAR, PAX3, STAT4, and YY1 (**Figure 6A**). In SK-OV-3 cells, AP-2, ATF2, IRF, and Nkx-2.5 were also significantly induced, whereas C/EBP, Ets PEA, MyoD, SMAD were not. LL-37 treatment of OVCAR-3 cells resulted in significant activation of HIF-1, MyoD, p53, STAT1, and STAT3, but not Ets PEA, IRF, and Nkx-2.5. The transcription factors that were not expressed in either cell line or not increased more than four fold by LL-37 included AP-1, androgen receptor (AR), Brn3, c-myb, E2F1, FKHR, HNF1, ISRE, MEF2, NF-1, NFAT, NF-E2, NF-κB, NF-Y, Oct, PAX5, RUNX AML, and STAT5 (data not shown).

Nuclear accumulation and activity of the transcription factors significantly enhanced in both ovarian cancer cell lines were also analyzed in SK-OV-3/FPRL1 KD-1, -2 cells and Ptx-

treated cells after LL-37 stimulation. CREB, ELK1, ER, GATA, and YY1 were inhibited in cells lacking FPRL1 as well as Ptx-treated cells, suggesting that LL-37 induces these transcription factors through FPRL1 signaling (**Figure 6B**). For each transcription factor examined, SK-OV-3/FPRL1 KD-1 cells exhibited more activity than FPRL1 KD-2 cells, which was consistent with qPCR data indicating that SK-OV-3/FPRL1 KD-1 cells express higher levels of the FPRL1 receptor. The activity of FAST1 and GR/PR were significantly reduced in FPRL1 KD-2 cells, but not in FPRL1 KD-1 cells or Ptx-treated cells, whereas STAT4 activity was significantly diminished only in Ptx-treated cells. These data suggest that LL-37 signals through both FPRL1-dependent and -independent pathways.

LL-37 modulates target gene expression through FPRL1 signaling.

To determine which genes are regulated by the LL-37-FPRL1 interaction in ovarian cancer cells, RNA was isolated from SK-OV-3 and OVCAR-3 cells after treatment with the peptide and analyzed by focused gene microarray. The expression profiles of 168 angiogenic and inflammatory genes were monitored after LL-37 treatment. Several of these genes were chosen for further validation by qPCR based on the magnitude of change in gene expression. These genes included *angiopoietin-like 3* (*angptl3*), *complement 5* (*c5*), *collagen type XVIII* (*col18a1*), *epidermal growth factor* (*egf*), *fibroblast growth factor 1* (*fgf1*), *fprl1*, and *hcap-18/ll-37*. The matrix metalloproteinases, *mmp2*, *9*, and *14*, as well as *urokinase plasminogen activator* (*upa*) were also analyzed in OVCAR-3 cells since we have previously shown that LL-37 increases their expression in SK-OV-3 cells. As shown in **Figure 7A**, LL-37 treatment resulted in the significant induction of the following genes in both cell lines: *c5, col18a1*, *egf*, *mmp2*, and *upa*. Gene expression of *angptl3* was significantly decreased in both cell lines. In SK-OV-3 cells, *fgf1* and *hcap-18/ll-37* expression was not affected by LL-37, whereas *fprl1* transcript was significantly more abundant. The peptide increased expression of *fgf1, fprl1, hcap-18/ll-37, mmp9* and *mmp14* in OVCAR-3 cells; although, only the *fgf1* induction was significant.

FPRL1's involvement in LL-37-stimulated gene expression was then assessed in knockdown and Ptx-treated cells. Expression of *c5, col18a1, mmp2* and *upa* were significantly repressed by the absence of FPRL1 signaling (**Figure 7B**). In contrast, *angptl3* expression was unaffected in SK-OV-3/FPRL1 KD cells or Ptx-treated cells. Ptx pretreatment significantly decreased *egf* expression by LL-37, but this effect was not observed in FPRL1 KD cells.

Work in Progress

Transforming growth factor β (TGF)1,3 expression in hMSCs.

Initially we measured TGFβ secretion from the conditioned medium to assess whether this known immune modulating factor might explain the ability of MSCs to recruit Tregs (**Figure 8**). TGFβ1, 2 and 3 was measured from the spent culture medium by luminex immunoassay as per manufacturer's recommendations (Luminex® Bead immunoassay Kit, LINCOplex from Millipore). The hMSCs were pre-treated for 1hr with LPS (TLR4) or poly(I:C) (TLR3), washed and cultured for an additional 48hrs prior to harvesting the spent medium for TGFβ detection. TLR3 activation of hMSCs considerably reduces (>80%) TGFβ1 and 3 secretion. No change was observed for TGFβ 2 after this treatment. LPS treatment led to little or no change over the untreated samples for this parameter (data not shown, n=3 with 4 different hMSC donors).

Immune repression by Indoleamine 2,3-dioxygenase (IDO) and prostaglandin E2 (PGE2) other known mediators of hMSC.

We have also measured other known potentiators of hMSCs immune modulation, IDO and PGE2 following LPS or poly(I:C)-treatment of hMSCs (**Figure 9)**. IDO was measured by real-time PCR analysis of RNA extracted from hMSCs treated for six-hours with the TLR ligands prior to RNA harvest. Data are presented by the quantitative comparative CT (threshold value) method (Coffelt, Waterman et al. 2008). PGE2 was measured from the spent culture medium

after 1 hr TLR-ligand pretreatment, wash and 48hrs of subsequent culture by commercially available ELISA assays. Consistent with the above results, it appears that these immunosuppressive indicators are elevated following TLR3 (poly(I:C)) activation and conversely mostly diminished by TLR4 (LPS) activation. n>3 with at least 4 different hMSC donors.

Ex vivo immune modulation of T cell activation is abrogated by TLR4 activation but maintained by TLR3 activation of hMSCs.

The immunosuppressive capability of hMSCs was established first by in vitro co-culture of the cells with human peripheral blood mononuclear cells (hPBMCs) or isolated T-cell subsets (Aggarwal and Pittenger 2005). One-hr TLR3 and TLR4 activated hMSCs were similarly co-cultured here with hPBMCs. For this purpose, hPBMCs or T-cell cultures were activated by phytohemagglutinin (PHA) prior to labeling with CFSE to monitor their activation or cell division and loaded at a 10:1 ratio over the treated hMSCs (**Figure 10)**. After greater than 72 hrs of co-culture the CFSE-labeled hPBMCs were harvested from the adherent hMSCs culture stained with propidium iodide and measured by flow cytometry. Unstained cells and hPBMCs not activated with PHA served as controls in the assay. Data are expressed as percent activation or change from the %activation obtained for the PHA-activated hPBMCs not co-cultured with hMSCs (Aggarwal and Pittenger 2005). As previously reported, incubation of untreated hMSCs with hPBMCs considerably reduced their activation (Aggarwal and Pittenger 2005). However, LPS-pretreatment inhibited this immune dampening effect by the hMSCs. Consistent with the data presented thus far, poly(I:C)-treatment maintained the immune dampening effect of the hMSCs. n>3 at least three different hMSC and hPBMC donors have been tested in this assay.

Task 2. To determine if tumor-derived LL-37 recruits regulatory T cells to the ovarian tumor microenvironment (Months 6-18):

a. SKOV3 human ovarian cancer cells will be stably transfected with an hCAP-18/LL-37-expressing plasmid then we will analyze these cells by Boyden and transwell migration assays.
b. *In vivo* migration assays will be performed by intravenous injection of labeled Tregs into immunocompromised mice that have established hCAP-18/LL-37-overexpressing or empty vector-transfected SKOV3 tumors.
c. In separate experiments, untransfected SKOV3 tumors will be established in immunocompromised mice then treated with a neutralizing LL-37 antibody or IgG control antibody followed by intravenous Tregs administration to demonstrate specificity of LL-37 effects.
d. Measure Tregs engraftment in tumors from all experiments by immunohistochemistry and flow cytometry assays.

Ovarian tumor-derived LL-37 functions as a chemoattractant for MSCs in vivo.

We established a collaboration with Dr. Frank Marini and Michael Andreef of MD Anderson Cancer Center who are experts in measuring MSCs engrafted into tumors by in vivo imaging techniques (Studeny, Marini et al. 2004). Human tumor xenografts were established in SCID mice by injection of OVCAR-3 ovarian cancer cells whose expression of hCAP-18/LL-37 was previously reported (Coffelt, Waterman et al. 2008). After 3.5 weeks, mice were randomly divided into two groups. One group (n = 11) was given an IgG control antibody and another group (n = 14) was given an anti-LL-37 antibody to neutralize the peptide's effect before injection of firefly luciferase (ffLUC)-labeled MSC. Bioluminescence images were taken throughout the experiment to monitor engraftment of MSC into the developing ovarian tumors. Neutralization of tumor-derived LL-37 in anti-LL-37 antibody-treated animals (αLL-37) abrogated the number of engrafted MSC into tumors when compared with IgG-treated animals. The

engraftment of the MSCs to the tumors was found to be diminished by the LL37 IgG treatment and further the tumor size was reduced and there was disruption of the tumor fibrovascular network as shown below. This data demonstrates our ability to develop the murine tumor models proposed here and gives support to the fact that MSCs in the ovarian tumor microenvironment promotes tumor growth.

Neutralization of tumor-derived LL-37 reduces tumor growth

Of the 11 tumor-bearing animals that received the IgG control antibody, 10 animals had visible tumors upon sacrifice. By contrast, 5 of the 14 animals given the anti-LL-37 antibody treatment regimen had no detectable tumor mass. Tumors from both groups were weighed after surgical removal and those from IgG. Inhibition of LL-37 significantly reduces engraftment of MSCs into ovarian tumors. Human ovarian tumor xenografts were established i.p. in SCID mice.

Mice were treated with IgG or anti-LL-37 antibodies (αLL-37) twice a week for 4 weeks. ffLUC-labeled MSCs were injected 4 times at weekly intervals 1day after the first weekly injection of antibody, then visualized by bioluminescence in live mice (**Figure 11)**. (A) Representative images of MSC engraftment into ovarian tumors 7 days after each injection of MSC. (B) Quantification of luminescence units emanating from tumorengrafted MSCs. Values are mean+/- SE. *P<0.05. (C) Expression of LL-37 (red) in ovarian tumor sections of IgG- and αL-37-treated mice. MSCs were identified using an anti-ffLUC antibody (green) and are indicated by white arrows. Nuclei were detected with DAPI. Sections are magnified X100. (Scale bar, 100μm.) (D) High-powered image (X400) of tumor section fluorescently labeled as described. (E) Sequential section of D immunohistochemically stained with anti-LL-37 antibodies followed by hematoxylin counterstain. (F) Example of LL-37-expressing MSCs in perivascular areas. (Scale bar, 50 μm, D–F.) treated animals were significantly larger than those from anti-LL-37-treated animals (98.43±13.51 mg vs. 46.39±12.65 mg, respectively; A).

To confirm these observations, tumors were stained for the proliferation marker Ki-67 (**Figure 12)**. A dramatic difference was again noted between tumors from IgG- and anti-LL-37-treated animals. Tumor nuclei of IgG-treated mice were almost all positive for Ki-67 in contrast to the few number of positive nuclei in tumors from LL-37 antibody-treated mice (B). Quantification of Ki-67+ nuclei in both treatment groups revealed a statistically significant difference (C). Notably, the stromal components of tumors from anti- LL-37-treated mice, including fibroblasts and endothelial cells, were absent in a large majority of areas (B; yellow arrows). Necrotic regions were also common in tumors from anti-LL-37-treated animals, but not in IgG-treated tumors. As shown in D, these necrotic areas stained positively for LL-37 suggesting that the peptide is sequestered in the debris.

MSC exposure to LL-37 promotes secretion of angiogenic and inflammatory molecules

It is well established that MSC produce many trophic factors with pro-tumorigenic functions (Karnoub, Dash et al. 2007; Tomchuck, Zwezdaryk et al. 2008; Uccelli, Moretta et al. 2008). Evidence from the *in vivo* experiments above indicated that MSC also produce LL-37. We tested conditioned medium from several MSC donor pools growing in culture by ELISA and found that these cells readily secrete the peptide (**Figure 13A**).

Next, we set out to determine how tumor-infiltrating MSC would react to the LL-37-rich microenvironment of ovarian tumors. We have previously reported that LL-37 enhances the secretion of interleukin (IL)-1β, IL-6, IL-8, IL-10, and tumor necrosis factor (TNF)-α from MSC while diminishing the secretion of IL-12(p70) (Tomchuck, Zwezdaryk et al. 2008). To identify additional MSC-derived cytokines and growth factors that may be regulated by ovarian tumor-derived LL-37 and expand our previous findings, conditioned medium from various LL-37-treated MSC donor pools was analyzed by Luminex-based assays. After 48 hours of LL-37 treatment, MSC were stimulated to release significantly more of the following cytokines when

compared with untreated cells: IL-1ra, IL-6, IL-10, IFNγ, CCL5 (RANTES), and VEGF (**Figure 13B**).

Conditioned medium was also analyzed for the presence and activation of matrix metalloproteinases (MMPs) by zymography assays. Untreated MSC secreted large amounts of the MMP-2 pro-form; no noticeable difference in expression was noted in the MMP-2 pro-form, regardless of treatment (upper band; **Figure 13C**). However, enzymatic activity of the active form of MMP-2 was increased after treatment of MSC with LL-37, EGF, and PMA (lower band; **Figure 13C, D**). MMP-9 activity was undetectable after any treatment and no expression was noted in casein gels indicating that MSC do not secrete measurable levels of stromelysins such as MMP-3 (data not shown).

We tested whether conditioned medium from LL-37-treated MSC—which contained larger amounts of pro-angiogenic factors, such as MMP-2, IL-6, and VEGF—could increase endothelial cell tubule formation *in vitro*. Serum-starved human umbilical vein endothelial cells (HUVECs) were seeded onto growth factor-reduced Matrigel in the presence of MSC conditioned medium. As shown in **Figure 13E**, all three donor pools of LL-37-treated MSC conditioned medium stimulated HUVECs to form tubules at a faster rate than medium from untreated MSC. HUVECs exposed to medium from LL-37-treated MSC began to migrate and organize into tube-like structures after only two hours. These data not only confirmed that LL-37-treated MSC conditioned medium contains increased amounts of pro-angiogenic molecules, they also confirmed that the pro-angiogenic milieu is functional and has bioactivity.

LL-37 increases the release of pro-tumorigenic molecules from ovarian cancer cells.

The soluble factors released from ovarian cancer cells after LL-37 treatment were also analyzed by a quantitative Luminex-based assay. Both LL-37-treated SK-OV-3 and OVCAR-3 cells produced significantly more CXCL10 (IP-10), EGF, and PDGF-BB when compared to untreated cells (**Figure 14A**). In addition, treatment of SK-OV-3 cells led to the increased secretion of IL-1ra, IL-9, and CCL2. Exposure of LL-37 to Ptx-treated SK-OV-3 cells, stably transfected NT cells, or SK-OV-3/FPRL1 KD cells significantly enhanced release of CXCL10 and EGF when compared to untreated cells (**Figure 14B**). However, LL-37 failed to stimulate PDGF-BB secretion in Ptx-treated and FPRL1 KD-2 cells. These data suggest that LL-37 utilizes FPRL1 for PDGF-BB release, but signals through another receptor(s) to increase CXCL10 and EGF release from ovarian cancer cells.

Work in Progress and Future Direction

The follow-up study that will be pursued builds on our recent reports that established that elevated levels of the human pro-inflammatory antimicrobial peptide LL-37 secreted from ovarian cancer cells recruit MSCs to the growing tumor. Enhanced levels of LL-37 in the ovarian tumors were also found to correlate with increased leukocyte infiltration. Further, these studies showed that MSCs are recruited to the ovarian tumors via engagement of their LL-37 receptor formyl receptor-like 1 (FPRL-1). Additionally, our work suggested that MSCs resident in the tumor microenvironment increased ovarian cancer growth and served to organize the fibrovascular networks within the tumor stroma. The proposed study is to define how MSCs affect the host immune-tumor microenvironment and recruits immunosuppressive cells. For this aim, labeled wild-type MSCs will be infused or not into mice bearing established ovarian tumors. We are developing an established murine ovarian cancer model or MOSEC model in our lab to compliment the expertise with human ovarian tumor xenograft models. The impact of the MSCs on tumor growth and spread will be measured from these two treatment groups and the changes in the specific immunosuppressive components will be analyzed from the tumor models. Thus, assays will be performed to detect known tumorassociated immune cells, including tumor-associated macrophages (TAMs), myeloid-derived suppressor cells (MDSCs),

vascular leukocytes (VLCs), dendritic cells (DCs), T regulatory cells (Tregs) and natural killer cells (NK) cells. Next, the immunosuppressive activity of these tumor-associated cells infused or not with MSCs will be assessed by established methods. The local MSC-mediated changes in the secretion of chemokines and cytokines will also be measured from these samples. Additional information may be gained by parallel studies employing infused fprl-1 knockout-MSCs that are impaired in their ability to migrate to the established ovarian tumors and therefore will not directly affect the tumor-associated immune components in the established microenvironment. Our study will also specifically target each of the identified critical immunosuppressive components affected by MSCs in the established murine tumor models and assess their impact on tumorigenesis. Recreate the tumor microenvironment supported by the MSCs through in vitro co-culture of ovarian cancer cells, tumor associated immune cells and MSCs and measure cancer cell growth and spread mechanisms. Systematically eliminate each component from this *in vitro* model and assess their impact on cancer cell growth and spread. The potential impact of altering the balance from permissive and supportive tumor microenvironments to one of tumor eradication in new treatment regimens is only beginning to be recognized. It is expected that the information gained from this study will potentially identify new therapeutic targets, provide new markers for earlier diagnoses of ovarian cancer and may establish new parameters that better predict the course of the disease.

KEY RESEARCH ACCOMPLISHMENTS:

We were the first to show that:

- LL-37 levels are highly elevated in ovarian cancer when compared to normal ovarian tissue.
- LL-37 specifically affects the growth and spread of ovarian cancer cells.
- LL37 in the ovarian cancer tumors specifically recruits mesenchymal stem cells (MSC).
- MSCs recruited to the cancer microenvironment promote tumor growth and spread by enhancing angiogenesis and secretion of growth factors but more importantly;
- MSCs recruited by LL-37 favor growth of ovarian tumors by supporting an immunosuppressive Tregs microenvironment

REPORTABLE OUTCOMES:

Publications

Suzanne L. Tomchuck, Kevin J. Zwezdaryk, Seth B. Coffelt, Ruth S. Waterman, and **Aline B. Scandurro.** Toll-Like Receptors on Human Mesenchymal Stem Cells Drive their Stress Signal Responses. Stem Cells. 2008 Jan;26(1):99-107. Epub 2007 Oct 4.

Seth B. Coffelt and **Aline B. Scandurro.** (2008) Tumors sound the alarmin(s). Cancer Res. Aug 15;68(16):6482-5.

Seth B. Coffelt, Ruth S. Waterman, Kevin J. Zwezdaryk, Kerstin Honer zu Bentrup, Suzanne L. Tomchuck, and **Aline B. Scandurro. (**2009) The human pro-inflammatory peptide, LL-37, recruits multipotent mesenchymal stem/progenitor cells to ovarian tumors and promotes their differentiation and immunomodulatory properties. Proc Natl Acad Sci U S A. 2009 Mar 10;106(10):3806-11. Epub 2009 Feb 20.

Seth B. Coffelt, Kevin J. Zwezdaryk, Suzanne L. Tomchuck, Elizabeth S. Danka, and **Aline B. Scandurro**. **(**2009) The antimicrobial peptide LL-37 utilizes the FPRL1 receptor on ovarian cancer cells to activate oncogenic signaling pathways and gene expression. Mol Cancer Res. 2009 Jun;7(6):907-15. Epub 2009 Jun 2.

Presentations

One poster "The role of human cationic antimicrobial protein 18 (hCAP-18), its derivative LL-37, and its receptor formyl peptide receptor like 1 (FPRL-1) in ovarian cancer " presented by my NCI-Fellowship funded minority Xavier Univ student at the American Association for Cancer Research Mtg. Colorado, April 09. One talk "LL37 and Ovarian Cancer" presented at Gordon Conference on Antimicrobial Peptides. Ventura CA 3/09.

Invited Talks: Pharmacology Spring '09. Pennington Biomedical Research Center Spring'09, Biomedical Engineering Spring '09. Pharmacology Spring '09. Louisiana Cancer Research Consortium, Summer'09. NIH NCI- Cancer and Inflammation Program section Frederick, MD 4/09.

Submitted Research Support

NIH RO1 04/01/10-3/31/14

Mesenchymal stem cells set-up an immunosuppressive microenvironment in ovarian cancers

The aims proposed are: *Aim 1.* Evaluate the specific immunosuppressive cell components affected by resident MSCs in the ovarian tumor microenvironment that favor tumor growth and spread.; *Aim 2.* Test the indirect contributions by resident MSCs on the immunosuppressive components of the ovarian tumor microenvironment and; *Aim 3.* Validate the established MSC-mediated immune cell interactions that lead to pro-tumor microenvironments.

Role: PI (70%) Direct costs for project: $250,000/year

NIH RO1 01/01/09-12/01/13

Pro-Inflammatory LL-37 and Mesenchymal Stem Cells in Ovarian Cancer

The goal of this project is to: (1) demonstrate that secreted LL-37 drives the recruitment and pro-angiogenesis potential of hMSC; (2) determine if hCAP-18/LL-37 expression is affected by hypoxia; (3) analyze the molecular interplay between ovarian tumor cells, peripheral blood mononuclear cells and mesenchymal stem cells that favors growth of ovarian tumor cells; (4) explore the principle that LL-37 is critical in ovarian cancer etiology by manipulation of its expression or the expression of its receptor within modified MSC delivered in a murine ovarian cancer xenograft model; and (5) delineate the role of LL-37 in ovarian tumor progression by manipulation of its expression within ovarian cancer cells engrafted in the murine xenograft model

Role: PI (50%) Direct costs for project: $250,000/year

Mary Kay Ash Award_ July 1, 2009 - June 30, 2011
Human Cationic Antimicrobial Peptide 18/LL-37: A New Biomarker for Ovarian Cancer
The goal of this proposal is to test the **hypothesis** that hCAP-18/LL-37 will serve as a new effective biomarker for the detection of early ovarian cancer disease.
Role: PI (15%) Direct costs for project: $100,000/2 yr

CONCLUSION:

A relatively recent therapeutic strategy in cancer treatments is targeting defective host immunity to tumors rather than the tumor itself. However, not enough is known about the important components that establish the defective immunity in cancer patients. In this proposal the potential contribution of bone marrow derived cells that are recruited by LL-37 to ovarian tumors was explored. Emerging evidence suggests that both resident and recruited bone marrow-derived cells play a critical and supportive role in creating a pro-tumorigenic host immune response. Indeed, an increased prevalence of recruited leukocytes in tumors correlates with a poor prognosis for the affected patient. By contrast, therapies that eradicate certain immune cells from the tumor microenvironment lead to longer remission periods for the treated patient. Along with other recruited cells, multipotent mesenchymal stromal cells (MSCs) formerly known as mesenchymal stem cells are also known to proceed from the bone marrow to tumors, and once there to reside within tumor stromal microenvironments. A few reports, including R. A. Weinberg's and ours, have demonstrated that this event favors breast and ovarian tumor growth and metastasis, respectively. However, to our knowledge, whether MSCs resident in this microenvironment help to establish a pro-tumorigenic host immune response remains to be tested. From the body of work done in this study it appears that LL-37 secreted from ovarian tumors serves to recruit MSCs that then preferentially support Tregs in the tumor microenvironment. It is expected that the information gained from this study will potentially identify new therapeutic targets, provide new markers for earlier diagnoses of ovarian cancer and may establish new parameters that better predict the course of the disease. This work has also allowed for the completion of several manuscripts (Coffelt and Scandurro 2008; Coffelt, Marini et al. 2009; Coffelt, Tomchuck et al. 2009) and the training of two graduate students and a minority undergraduate student. It has also provided essential preliminary data for three grant applications.

REFERENCES:

Aggarwal, S. and M. F. Pittenger (2005). "Human mesenchymal stem cells modulate allogeneic immune cell responses." Blood **105**(4): 1815-22.

Bowdish, D. M., D. J. Davidson, et al. (2004). "The human cationic peptide LL-37 induces activation of the extracellular signal-regulated kinase and p38 kinase pathways in primary human monocytes." J Immunol **172**(6): 3758-65.

Carretero, M., M. J. Escamez, et al. (2008). "In vitro and in vivo wound healing-promoting activities of human cathelicidin LL-37." J Invest Dermatol **128**(1): 223-36.

Coffelt, S. B., F. C. Marini, et al. (2009). "The pro-inflammatory peptide LL-37 promotes ovarian tumor progression through recruitment of multipotent mesenchymal stromal cells." Proc Natl Acad Sci U S A **106**(10): 3806-11.

Coffelt, S. B. and A. B. Scandurro (2008). "Tumors sound the alarmin(s)." Cancer Res **68**(16): 6482-5.

Coffelt, S. B., S. L. Tomchuck, et al. (2009). "Leucine leucine-37 uses formyl peptide receptor-like 1 to activate signal transduction pathways, stimulate oncogenic gene expression, and enhance the invasiveness of ovarian cancer cells." Mol Cancer Res **7**(6): 907-15.

Coffelt, S. B., R. S. Waterman, et al. (2008). "Ovarian cancers overexpress the antimicrobial protein hCAP-18 and its derivative LL-37 increases ovarian cancer cell proliferation and invasion." Int J Cancer **122**(5): 1030-9.

Coffelt, S. B., R. S. Waterman, et al. (2008). "Ovarian cancers overexpress the antimicrobial protein hCAP-18 and its derivative LL-37 increases ovarian cancer cell proliferation and invasion." Int J Cancer **122**(5): 1030-9.

Heilborn, J. D., M. F. Nilsson, et al. (2005). "Antimicrobial protein hCAP18/LL-37 is highly expressed in breast cancer and is a putative growth factor for epithelial cells." Int J Cancer **114**(5): 713-9.

Karnoub, A. E., A. B. Dash, et al. (2007). "Mesenchymal stem cells within tumour stroma promote breast cancer metastasis." Nature **449**(7162): 557-63.

Koczulla, R., G. von Degenfeld, et al. (2003). "An angiogenic role for the human peptide antibiotic LL-37/hCAP-18." J Clin Invest **111**(11): 1665-72.

Nakamizo, A., F. Marini, et al. (2005). "Human bone marrow-derived mesenchymal stem cells in the treatment of gliomas." Cancer Res **65**(8): 3307-18.

Studeny, M., F. C. Marini, et al. (2004). "Mesenchymal stem cells: potential precursors for tumor stroma and targeted-delivery vehicles for anticancer agents." J Natl Cancer Inst **96**(21): 1593-603.

Tjabringa, G. S., J. Aarbiou, et al. (2003). "The antimicrobial peptide LL-37 activates innate immunity at the airway epithelial surface by transactivation of the epidermal growth factor receptor." J Immunol **171**(12): 6690-6.

Tjabringa, G. S., D. K. Ninaber, et al. (2006). "Human cathelicidin LL-37 is a chemoattractant for eosinophils and neutrophils that acts via formyl-peptide receptors." Int Arch Allergy Immunol **140**(2): 103-12.

Tokumaru, S., K. Sayama, et al. (2005). "Induction of keratinocyte migration via transactivation of the epidermal growth factor receptor by the antimicrobial peptide LL-37." J Immunol **175**(7): 4662-8.

Tomchuck, S. L., K. J. Zwezdaryk, et al. (2008). "Toll-like receptors on human mesenchymal stem cells drive their migration and immunomodulating responses." Stem Cells **26**(1): 99-107.

Uccelli, A., L. Moretta, et al. (2008). "Mesenchymal stem cells in health and disease." Nat Rev Immunol **8**(9): 726-36.

Viswanathan, A., R. G. Painter, et al. (2007). "Functional expression of N-formyl peptide receptors in human bone marrow-derived mesenchymal stem cells." Stem Cells **25**(5): 1263-9.

von Haussen, J., R. Koczulla, et al. (2008). "The host defence peptide LL-37/hCAP-18 is a growth factor for lung cancer cells." Lung Cancer **59**(1): 12-23.

Yang, D., Q. Chen, et al. (2000). "LL-37, the neutrophil granule- and epithelial cell-derived cathelicidin, utilizes formyl peptide receptor-like 1 (FPRL1) as a receptor to chemoattract human peripheral blood neutrophils, monocytes, and T cells." J Exp Med **192**(7): 1069-74.

SUPPORTING DATA:

Figure 1. *LL-37 mediates MSC migration and invasion through a G protein-coupled receptor*. (A) FPRL1 expression on three different donor pools of MSC analyzed by flow cytometry. (B) Graphic representation of MSC migration stimulated as indicated in a modified Boyden chamber. EGF and PMA were used at 10 ng/mL. (C) MSC migration after pretreatment of cells with 100 ng/mL pertussis toxin (Ptx), or pre-incubation of LL-37 and EGF with an ant-LL-37 neutralizing antibody (αLL-37). (D) Invasion of MSC through Matrigel-coated inserts following stimulation as indicated. (E) MSC invasion after pretreatment of cells with Ptx, or preincubation of LL-37 and EGF with αLL-37 antibody. (F) Lysates from LL-37-treated MSC analyzed for ERK phosphorylation by Western blot. MSC in far right lane were pretreated with Ptx for 1 hour before stimulation with LL-37 for 10 minutes. M = molecular weight marker. (G) Quantification of Western blot band intensity by densitometry (n =3), plotted as a bar graph.

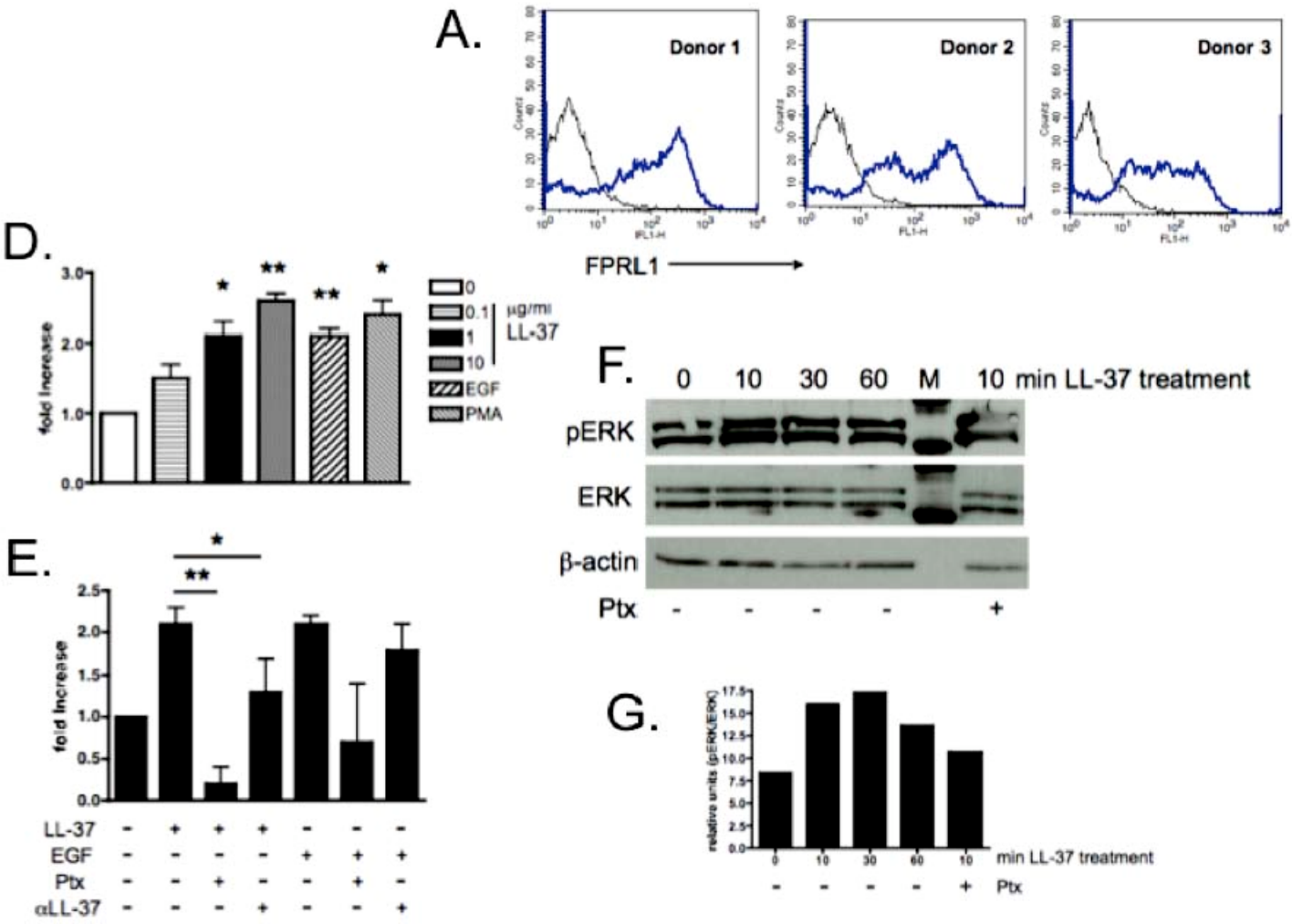

Figure 2. *FPRL1 is expressed on ovarian cancer cells*. Ovarian cancer cell lines, representing different histological subtypes, were analyzed for FPRL1 expression by flow cytometry. Primary antibodies were detected with Alexa-488-conjugated goat anti-rabbit antibodies. Blue line represents FPRL1 expression and black line represents isotype control. n = 3

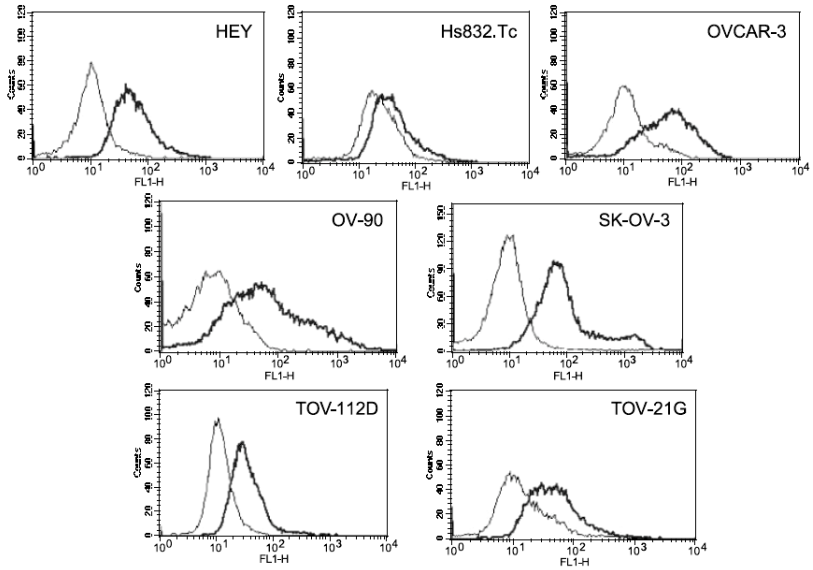

Figure 3. *LL-37 does not signal through a G protein-coupled receptor, such as FPRL1, to stimulate ovarian cancer cell proliferation.* Graphic representation of ovarian cancer cell growth after 48 hour exposure to LL-37 or EGF. Serum-starved cells were pretreated with or without 10 ng/mL pertussis toxin (Ptx) for 1 hour, followed by LL-37 or EGF treatment. After 48 hours, cellular DNA was measured using fluorescent probes. MFI = mean fluorescence intensity. Values are mean ± SE of three or more independent experiments. Each cell line was assayed a minimum of three times.

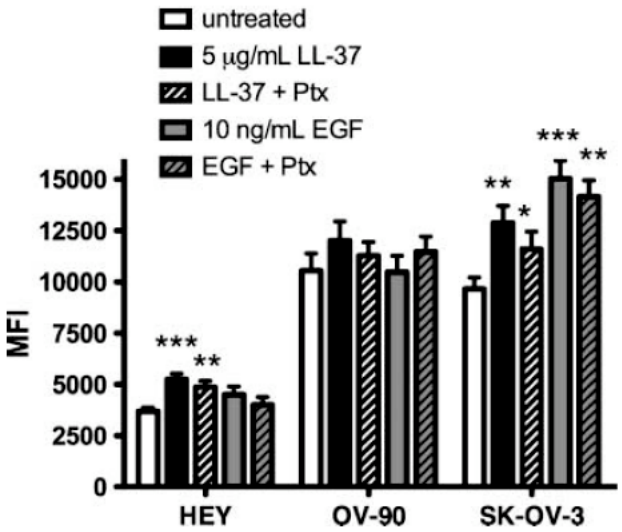

Figure 4. *LL-37 mediates ovarian cancer cell migration and invasion through FPRL1***.** (**A**) Graphic representation of ovarian cancer cell migration. Serum-starved cells were pretreated with or without 10 ng/mL pertussis toxin (Ptx) for 1 hour, then loaded into a modified Boyden chamber containing 1 µg/mL LL-37 or 10 ng/mL EGF. Columns represent the mean fold change ± SE of the number of migrated cells compared to unstimulated controls. (**B**) Graph depicting *fprl1* gene expression in knockdown (KD) cells. SK-OV-3 cells stably-transduced with lentiviruses containing FPRL1-specific shRNA (called KD-1 through 5) or non-target (NT) sequences were analyzed by qPCR. Values are mean ± SE of three independent experiments compared to NT cells. (**C**) Graphic representation of ovarian cancer cell invasion. Ptx-treated SK-OV-3 cells, SK-OV-3 NT cells, and SK-OV-3/FPRL1 KD-2 cells were seeded onto Matrigel-coated inserts in medium containing 10 µg/mL LL-37 or 10 ng/mL EGF. After incubation, cells were fluorescently labeled and relative fluorescence units were obtained. Columns represent the mean fold change ± SE of the mean fluorescence intensity of invaded cells compared to unstimulated controls. **p* < 0.05, ***p* < 0.01.

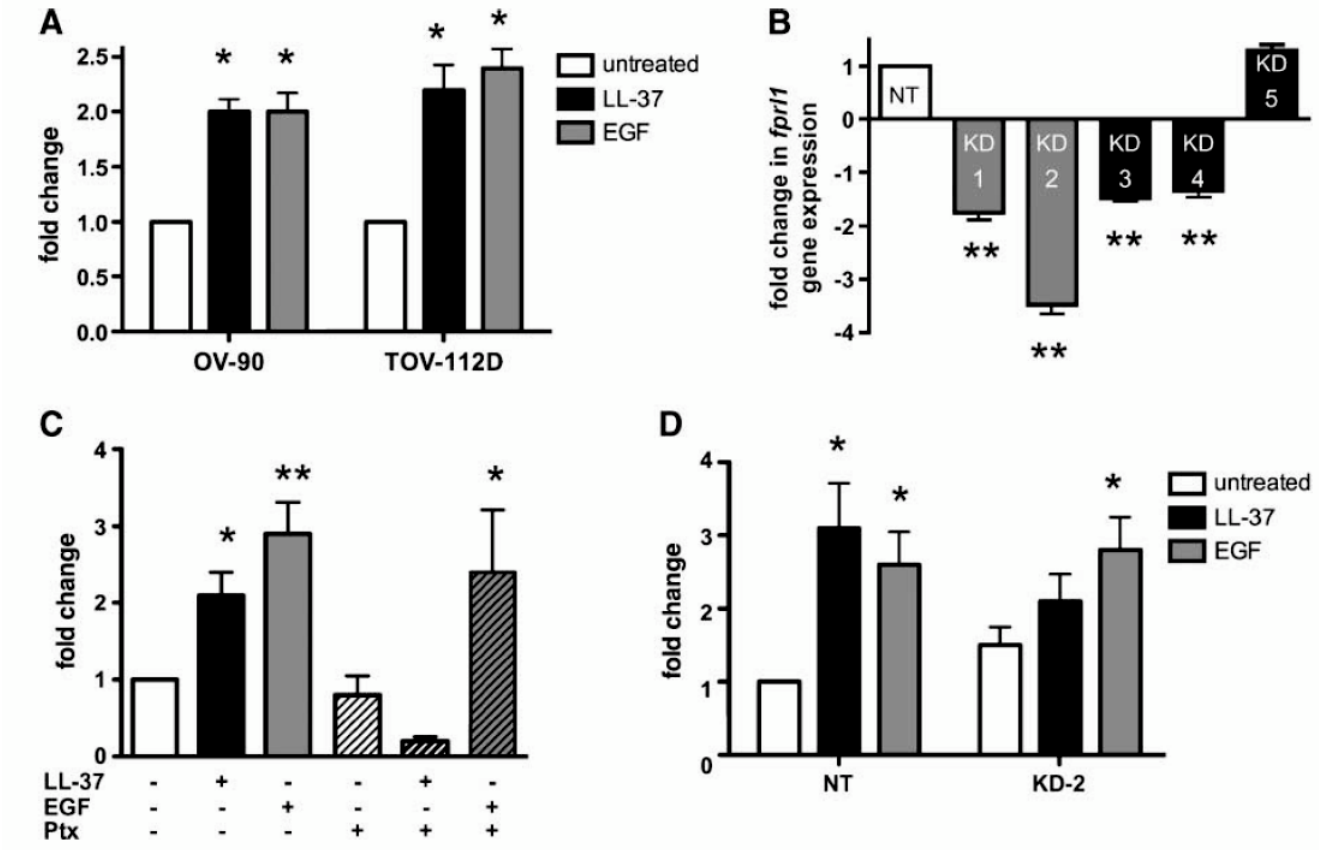

Figure 5. *Activation of MAPK signaling pathways by LL-37 does not occur through FPRL1.* (**A**) The influence of recombinant LL-37 (5 µg/mL) on phosphorylation of AKT, ERK, and STAT3 in SK-OV-3 cells. Images are representative of three or more independent experiments. (**B**) Cellular protein was isolated from Ptx-treated SK-OV-3 cells, SK-OV-3 NT cells, and SK-OV-3/FPRL1 KD-2 cells that were treated with LL-37 for 30 min. Phosphorylation and expression of

ERK was measured by Western blot analysis. β-actin levels were assessed to ensure equal loading.

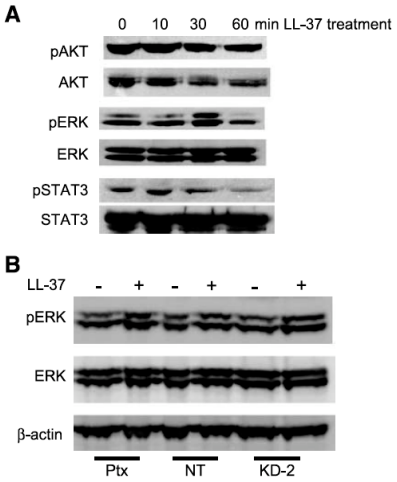

Figure 6. *Inhibition of FPRL1 negatively affects LL-37-induced nuclear accumulation and activity of multiple transcription factors.* (**A**) Graphic representation of transcription factor-DNA binding. Nuclear extracts from serum-starved ovarian cancer cells treated or untreated with 5 μg/mL LL-37 for 1 hour were analyzed for transcription factors bound to specific fluorescently-labeled oligonucleotide probes. MFI = mean fluorescence intensity. Columns are mean ± SE. (**B**) Analysis of transcription factor activity in SK-OV-3/FPRL1 KD and Ptx-treated cells after LL-

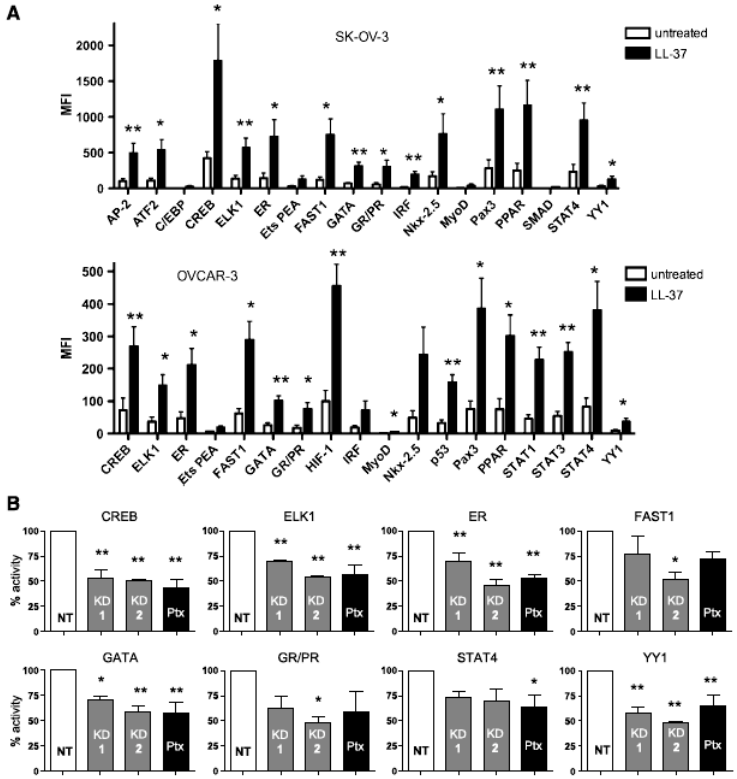

37 treatment as described above. Columns are mean ± SE of four independent experiments. *$p < 0.05$, **$p < 0.01$.

Figure 7. *LL-37 modulates target gene expression through FPRL1 signaling.* (**A**) Graphic representation of genes regulated by LL-37. Serum-starved SK-OV-3 and OVCAR-3 cells were treated with 5 µg/mL LL-37 for 6 hours. RNA was isolated and analyzed by qPCR using the delta Ct method. (**B**) Analysis of target gene expression in SK-OV-3/FPRL1 KD and Ptx-treated cells after LL-37 treatment. Columns are mean ± SE of three or more independent experiments. *$p < 0.05$, **$p < 0.01$.

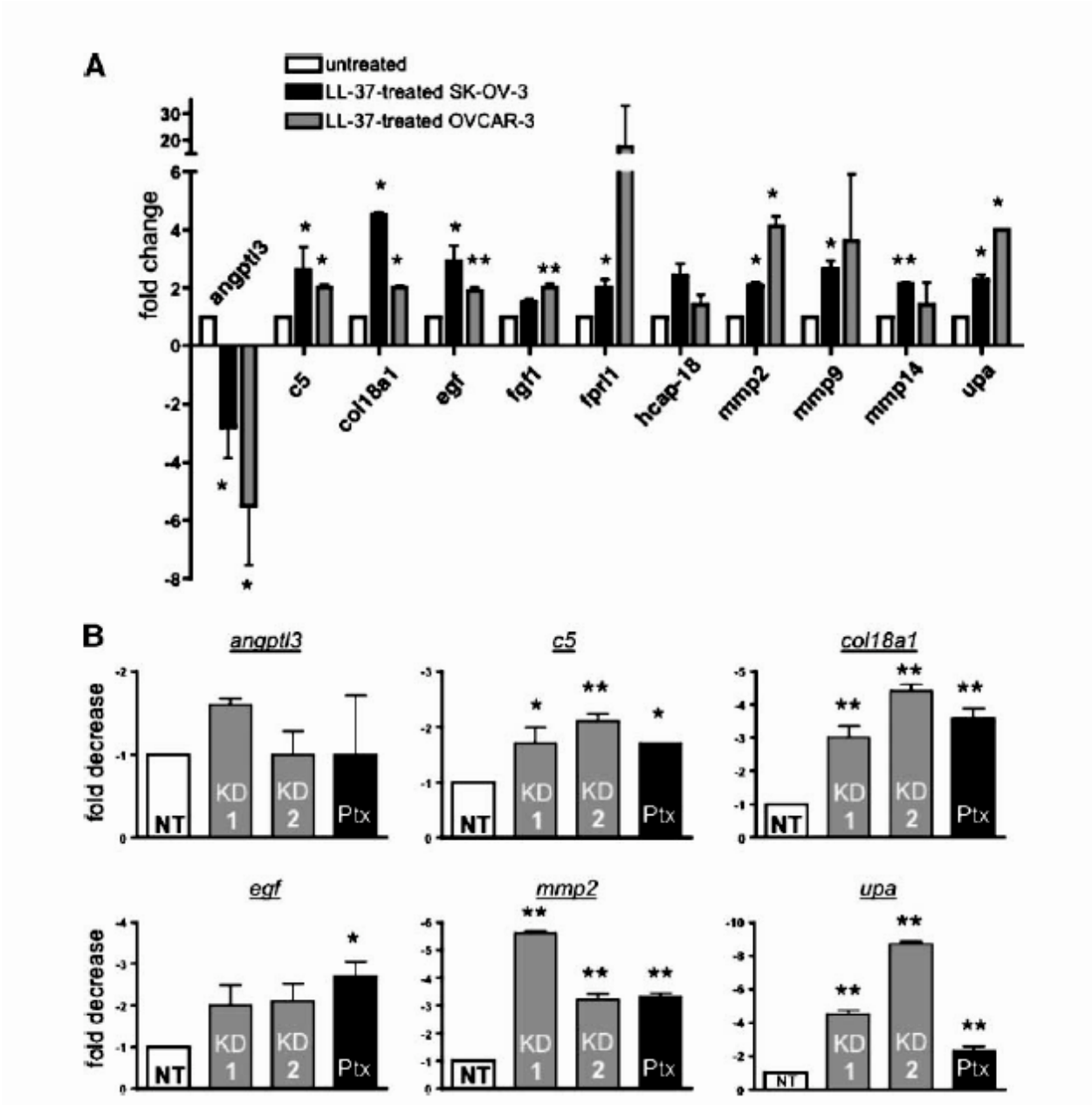

Figure 8. *Transforming growth factor β (TGF)1,3 expression in hMSCs.* The hMSCs were pre-treated for 1hr with LPS or poly(I:C), washed and cultured for an additional 48hrs prior to harvesting the spent medium for TGFβ detection. TGFβ1, 2 & 3 was measured from the spent culture medium by luminex immunoassay as per manufacturer's recommendations (Luminex® Bead immunoassay Kit, LINCOplex from Millipore). TGFβ1, 2 & 3 was measured from the spent culture medium by luminex immunoassay as per manufacturer's recommendations (Luminex® Bead immunoassay Kit, LINCOplex from Millipore).

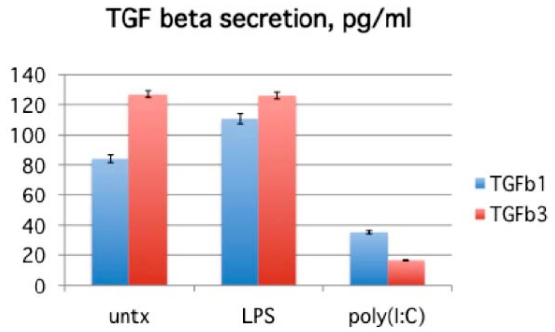

Figure 9. *Immune repression by Indoleamine 2,3-dioxygenase (IDO) and prostaglandin E2 (PGE2) other known mediators of hMSC.*
The levels of immune modulating factors indoleamine 2,3-dioxygenase (IDO) and prostaglandin E2 (PGE2) also differ in TLR3 and TLR4 activated hMSCs. The hMSCs were pre-treated for 1hr with LPS or poly(I:C), washed and cultured for an additional 48hrs prior to harvesting the spent medium for PGE2 secretion(B). For IDO measurements hMSCs were treated for six hours prior to harvesting the RNA and real time PCR assay (A). Data are presented by the quantitative comparative CT (threshold value) method.

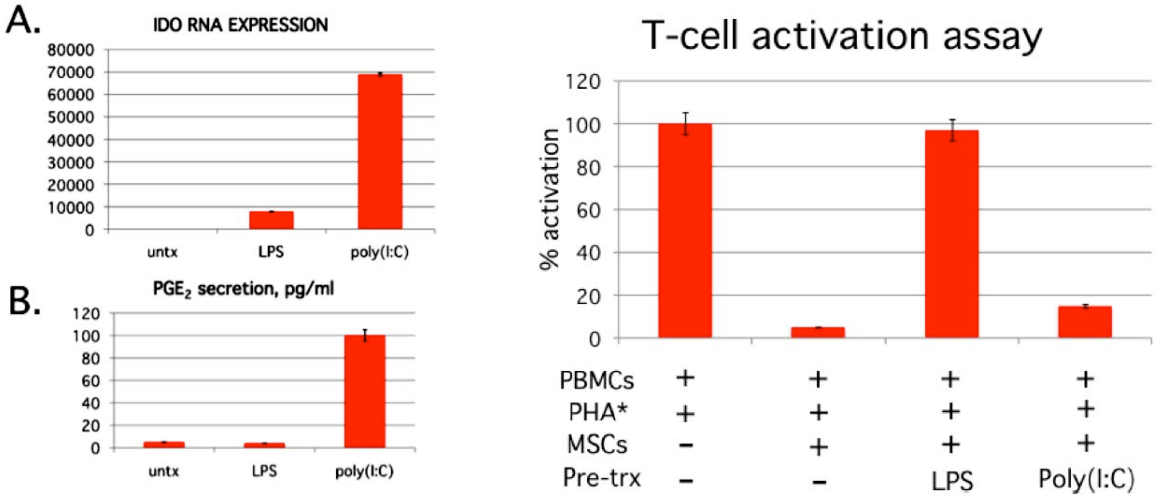

Figure 10. *Ex vivo immune modulation of T cell activation is abrogated by TLR4 activation but maintained by TLR3 activation of hMSCs.*TLR4 activation of hMSCs inhibits their established ex vivo immunosuppression. Human peripheral blood mononuclear cells (hPBMCs) or T-cell

cultures were activated by phytohemagglutinin (PHA*, 2.5 ng/mL) prior to labeling with CFSE to monitor their activation or cell division and loaded at a 10:1 ratio over the treated hMSCs. The hMSCs were pretreated for 1 hr with TLRligands, washed in medium and loaded with the hPBMCs. After greater than 72 hrs of co-culture the CFSE-labeled hPBMCs were harvested from the adherent hMSCs culture stained with propidium iodide and measured by flow cytometry. Unstained cells and hPBMCs not activated with PHA served as controls in the assay. Data are expressed as percent activation or change from the %activation obtained for the PHA-activated hPBMCs not co-cultured with hMSCs.

Figure 11. *Inhibition of LL-37 significantly reduces engraftment of MSC into ovarian tumors.* Human ovarian tumor xenografts were established i.p. in SCID mice. Mice were treated with IgG or anti-LL-37 antibodies (αLL-37) twice a week for 4 weeks. Firefly luciferase (ffLUC)-labeled MSC were injected 4 times at weekly intervals 1 day after the first weekly injection of antibody then visualized by bioluminescence in live mice. (**A**) Representative images of MSC engraftment into ovarian tumors, 7 days after each injection of MSC. (**B**) Quantification of luminescence units emanating from tumor-engrafted MSC. Values are mean ± SE. *$p < 0.05$. (**C**) Expression of LL-37 (red) in ovarian tumor sections of IgG- and αLL-37-treated mice. MSC were identified using an anti-ffLUC antibody (green) and are indicated by white arrows. Nuclei were detected with DAPI. Sections are magnified 100X. Scale bar denotes 100 μm. (**D**) High powered image (400X) of tumor section fluorescently labeled as above. (**E**) Sequential section of panel D immunohistochemically stained with anti-LL-37 antibodies followed by hematoxylin counterstain. (**F**) Example of LL-37-expressing MSC in perivascular areas. Scale bar denotes 50 μm for panels D-F.

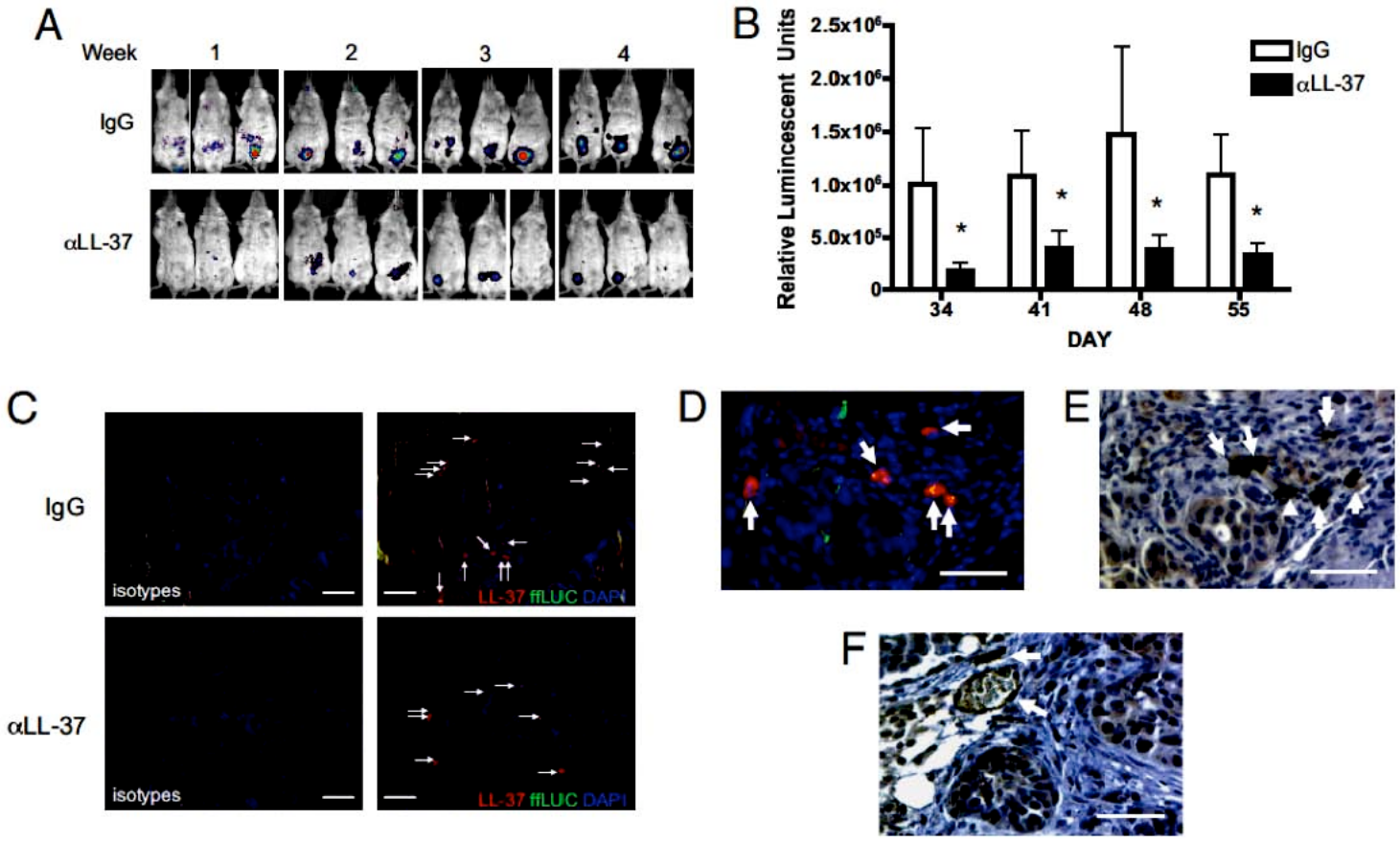

Figure 12. *Growth of ovarian tumor xenografts is diminished by neutralization of LL-37***.** (**A**) Graphic representation of tumor weights from IgG- (n = 10) and αLL-37-treated (n = 9) animals obtained after surgical removal. Values are mean ± SE. ***p* < 0.01. (**B**) Representative images of tumors stained for Ki-67 with hematoxylin counterstain. Arrows indicate mouse stroma in human xenograft tumors. Scale bar denotes 50 µm. (**C**) Graphic representation of the average number of Ki-67^{+} nuclei per high-powered field (HPF). Values are mean ± SE. ***p* < 0.01. (**D**) Expression of Ki-67 and LL-37 in tumor necrotic region from an αLL-37-treated mouse. Scale bar denotes 100 µm.

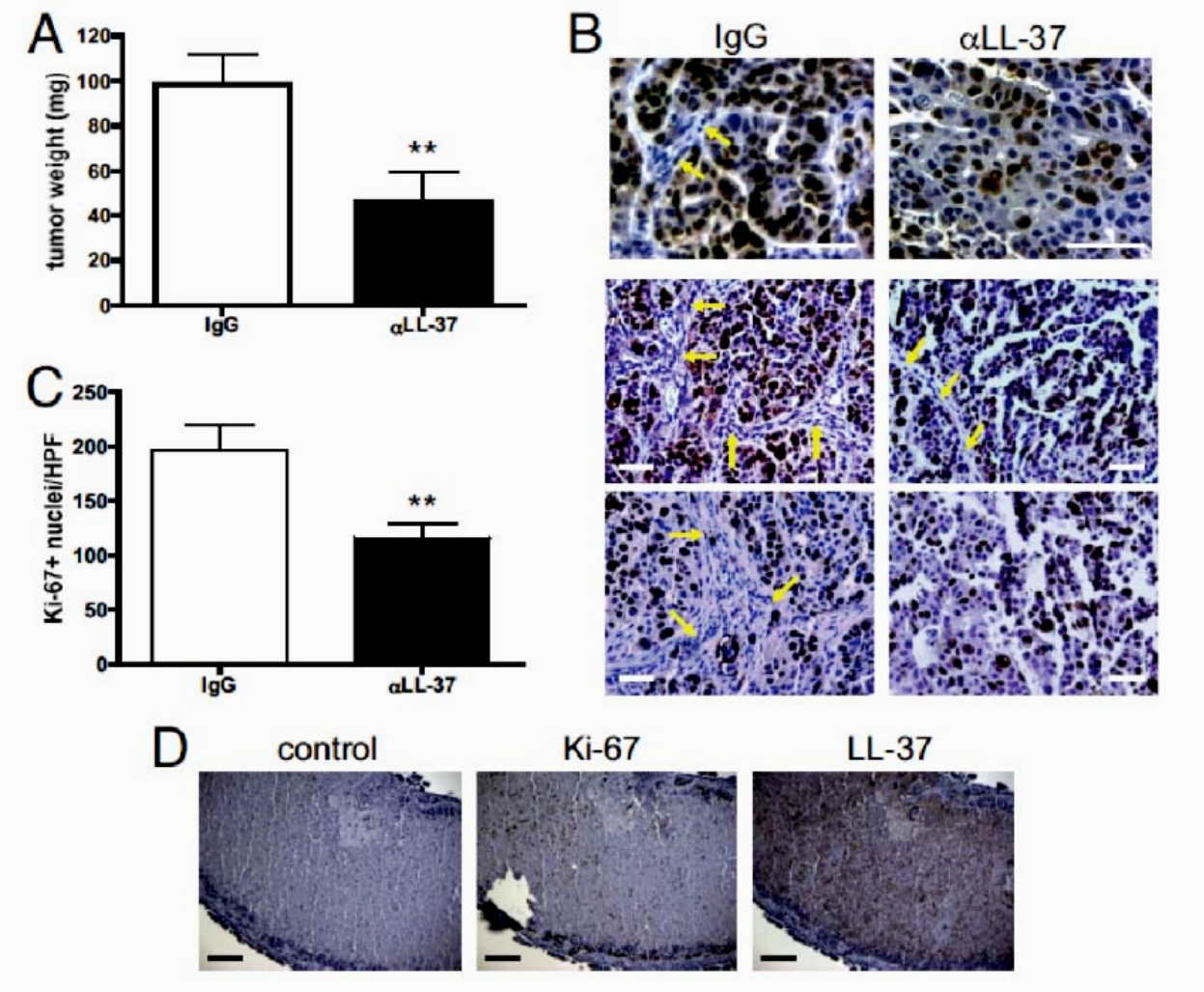

Figure 13. *MSC secrete increased levels of angiogenic and inflammatory mediators after LL-37 stimulation.* (**A**) The concentration of LL-37 in conditioned medium taken from unstimulated MSC in culture. (**B**) Serum-starved MSC were treated with 5 µg/mL LL-37 for 48 hours then conditioned medium was analyzed by Luminex-based cytokine arrays. Values are mean ± SE. **p* < 0.05, ***p* < 0.01. (**C**) Analysis of MSC conditioned medium after treatment for 48 hours as indicated by gelatin zymography. The representative image depicts the electrophorectic pro-MMP-2 (72 kDa) and active MMP-2 (62 kDa). MMP-9 (92 kDa) was not undetectable. (**D**) Quantification of zymography by densitometry. Intensity of the lower band (active MMP-2, 62

kDa) is plotted as a bar graph (n = 3). (**E**) Conditioned medium from untreated and LL-37-treated MSC was added to human umbilical vein endothelial cells (HUVECs) then seeded onto Matrigel. Fluorescently labeled cells were monitored were for formation of capillary-like tubules. Photographs are representative of HUVECs after 2 hours incubation.

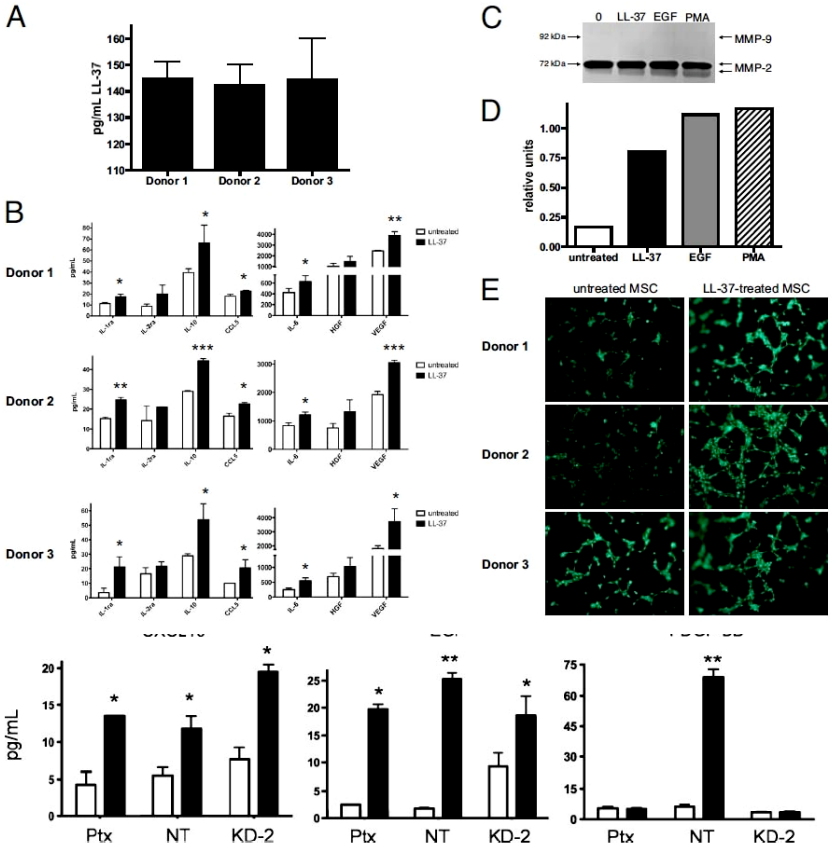

Figure 14. *LL-37 increases the release of pro-tumorigenic molecules from ovarian cancer cells.* (**A**) Serum-starved ovarian cancer cells were treated with 5 µg/mL LL-37 for 48 hours then conditioned medium was analyzed by Luminex-based cytokine arrays. The amount of cytokines and growth factors in conditioned medium is represented graphically. (**B**) Ptx-treated SK-OV-3 cells, SK-OV-3 NT cells, and SK-OV-3/FPRL1 KD-2 cells were treated with LL-37 as above. The levels of EGF, CXCL10, and PDGF-BB were measured in conditioned medium after 48 hours. Columns are mean ± SE of three or more independent experiments. **p* < 0.05, ***p* < 0.01, ****p* < 0.001.

APPENDICES: Attach all appendices that contain information that supplements, clarifies or supports the text. Examples include original copies of journal articles, reprints of manuscripts and abstracts, a curriculum vitae, patent applications, study questionnaires, and surveys, etc.

Personnel that worked on the study include graduate student Suzanne Tomchuck, research assistant Sarah Henkle and Seth Coffelt, PhD.

2 reprints follow- PNAS 6 pages and Mol Can Research 9 pages

The pro-inflammatory peptide LL-37 promotes ovarian tumor progression through recruitment of multipotent mesenchymal stromal cells

Seth B. Coffelt[a], Frank C. Marini[b], Keri Watson[b], Kevin J. Zwezdaryk[c], Jennifer L. Dembinski[b], Heather L. LaMarca[d], Suzanne L. Tomchuck[c], Kerstin Honer zu Bentrup[c], Elizabeth S. Danka[c], Sarah L. Henkle[c], and Aline B. Scandurro[c,1]

[a]Tumor Targeting Group, University of Sheffield School of Medicine, Sheffield, United Kingdom; [b]Department of Stem Cell Transplant and Cellular Therapy, University of Texas M. D. Anderson Cancer Center, Houston, TX; and [c]Department of Microbiology and Immunology, Tulane University, New Orleans, LA; and [d]Department of Molecular & Cellular Biology, Baylor College of Medicine, Houston, TX

Communicated by Darwin J. Prockop, Tulane University, New Orleans, LA, January 9, 2009 (received for review April 22, 2008)

Bone marrow-derived mesenchymal stem cells or multipotent mesenchymal stromal cells (MSCs) have been shown to engraft into the stroma of several tumor types, where they contribute to tumor progression and metastasis. However, the chemotactic signals mediating MSC migration to tumors remain poorly understood. Previous studies have shown that LL-37 (leucine, leucine-37), the C-terminal peptide of human cationic antimicrobial protein 18, stimulates the migration of various cell types and is overexpressed in ovarian, breast, and lung cancers. Although there is evidence to support a pro-tumorigenic role for LL-37, the function of the peptide in tumors remains unclear. Here, we demonstrate that neutralization of LL-37 in vivo significantly reduces the engraftment of MSCs into ovarian tumor xenografts, resulting in inhibition of tumor growth as well as disruption of the fibrovascular network. Migration and invasion experiments conducted in vitro indicated that the LL-37-mediated migration of MSCs to tumors likely occurs through formyl peptide receptor like-1. To assess the response of MSCs to the LL-37-rich tumor microenvironment, conditioned medium from LL-37-treated MSCs was assessed and found to contain increased levels of several cytokines and pro-angiogenic factors compared with controls, including IL-1 receptor antagonist, IL-6, IL-10, CCL5, VEGF, and matrix metalloproteinase-2. Similarly, Matrigel mixed with LL-37, MSCs, or the combination of the two resulted in a significant number of vascular channels in nude mice. These data indicate that LL-37 facilitates ovarian tumor progression through recruitment of progenitor cell populations to serve as pro-angiogenic factor-expressing tumor stromal cells.

FPRL1 | hCAP-18 | mesenchymal stem cell | ovarian cancer | tumor engraftment

Histological examination of ovarian, breast, and lung tumors has shown that the pro-inflammatory peptide LL-37 (leucine, leucine-37) is up-regulated in these malignancies (1–3). LL-37 was originally identified as a component of host defense peptides released by innate immune cells to combat microorganisms (4–6). However, recent investigations have revealed more complex and diverse functions of the peptide (7–9). LL-37 is synthesized as the 37-aa C terminus of human cationic antimicrobial protein 18 (hCAP-18) and maintained in an inactive state until release by enzymatic cleavage (4, 5, 10–12). Expression and secretion of LL-37 is elevated at sites of inflammation and wound healing, where the peptide functions as a proliferative signal and pro-angiogenic factor (7–9). The peptide also acts as a potent chemoattractant for various immune cells through activation of formyl peptide receptor like-1 (FPRL1) (13, 14). In contrast to LL-37's established functions in host defense and tissue damage, the role of the peptide in the tumor microenvironment and the advantage given to tumor cells by its overexpression is not entirely clear.

The heterogeneous population of progenitor cells known as multipotent stromal cells or mesenchymal stem cells (MSC) has been shown to engraft within tumor microenvironments, where they incorporate into the stroma of solid tumors as tumor-associated fibroblasts or pericyte-like cells and potentiate tumor progression through the release of paracrine signals (15–25). Kaposi sarcoma seems to be the only exception to this phenomenon, as MSCs inhibit the growth of this tumor type (23). However, the tropism of MSCs for Kaposi sarcoma is maintained, suggesting that the factors responsible for MSC recruitment to tumors are commonly secreted by multiple tumors of different tissue origin. In fact, a number of soluble factors have been implicated in MSC migration to tumors, including many of the same inflammatory mediators up-regulated in injured and inflamed tissues (17, 18, 20, 26–28). Therefore, given the similar expression pattern of LL-37 in tumors, damaged tissue, and inflammation, where MSCs are prominent, as well as the ability of the peptide to stimulate chemotaxis of various cell types, we hypothesized that ovarian tumor-derived LL-37 recruits MSCs to the tumor microenvironment to support cancer progression.

Results

LL-37 Promotes Migration and Invasion of MSC in Vitro. As LL-37 has been shown to activate migration through the FPRL1 receptor in various cell types, several donor pools of MSCs were examined for expression of FPRL1 (13). Flow cytometry analyses confirmed the expression of FPRL1 on all MSC donor pools, corroborating results from other laboratories (Fig. 1*A*) (29).

We extended our previous findings to determine the optimal dosage of the peptide using in vitro chemotaxis assays (26). As shown in Fig. 1*B*, LL-37 induced the migration of MSCs in a dose-dependent manner, and the peptide performed as well as EGF, an established chemotactic factor for these cells (17). MSCs were pretreated with pertussis toxin (Ptx), a $G_{\alpha i}$ inhibitor, before activation with LL-37 or EGF to prevent FPRL1 signaling. Ptx treatment followed by LL-37 stimulation resulted in a significant inhibition of MSC migration, whereas no significant difference was observed between EGF-stimulated, Ptx-treated cells and EGF-stimulated cells alone (Fig. 1*C*). LL-37 and EGF were also preincubated with a neutralizing LL-37 antibody and, as expected, the neutralizing antibody (αLL-37) abolished LL-37's chemotactic effects on MSCs but had no effect on EGF-stimulated cells (Fig. 1*C*). No decrease in MSC migration was observed in wells with a control IgG antibody (data not shown).

MSC invasion through Matrigel-coated inserts was also sig-

Author contributions: S.B.C., F.C.M., K.J.Z., and A.B.S. designed research; S.B.C., F.C.M., K.W., K.J.Z., J.L.D., H.L.L., S.L.T., K.H.z.B., E.S.D., S.L.H., and A.B.S. performed research; S.B.C., F.C.M., K.J.Z., H.L.L., S.L.T., and A.B.S. analyzed data; and S.B.C., F.C.M., and A.B.S. wrote the paper.

The authors declare no conflict of interest.

[1]To whom correspondence should be addressed. E-mail: alibscan@tulane.edu.

This article contains supporting information online at www.pnas.org/cgi/content/full/0900244106/DCSupplemental.

www.pnas.org/cgi/doi/10.1073/pnas.0900244106

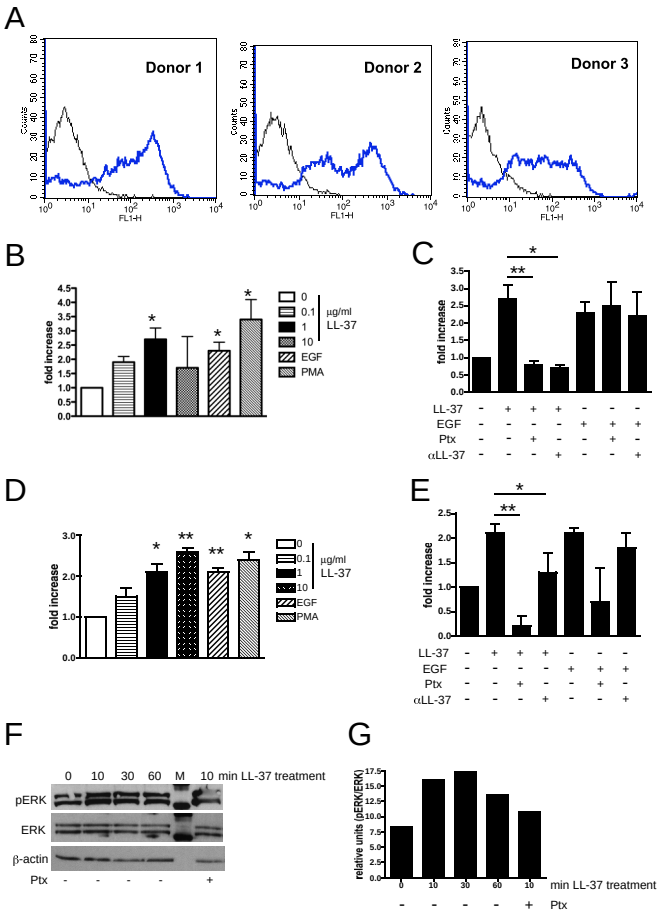

Fig. 1. LL-37 mediates MSC migration and invasion through a G protein-coupled receptor. (*A*) FPRL1 expression on 3 different donor pools of MSCs analyzed by flow cytometry. (*B*) Graphic representation of MSC migration stimulated as indicated in a modified Boyden chamber. EGF and PMA were used at 10 ng/mL. (*C*) MSC migration after pretreatment of cells with 100 ng/mL pertussis toxin (Ptx), or preincubation of LL-37 and EGF with an anti-LL-37 neutralizing antibody (αLL-37). (*D*) Invasion of MSCs through Matrigel-coated inserts following stimulation as indicated. (*E*) MSC invasion after pretreatment of cells with Ptx or preincubation of LL-37 and EGF with αLL-37 antibody. *, $P < 0.05$; **, $P < 0.01$. (*F*) Lysates from LL-37-treated MSCs analyzed for ERK phosphorylation by Western blot. MSCs in the far right lane were pretreated with Ptx for 1 h before stimulation with LL-37 for 10 min. M = molecular weight marker. (*G*) Quantification of Western blot band intensity by densitometry ($n = 3$), plotted as a bar graph.

nificantly enhanced by LL-37 stimulation (Fig. 1*D*). Pretreatment of MSC with Ptx significantly attenuated LL-37's ability to promote invasion (Fig. 1*E*). EGF-stimulated cells were slightly affected by Ptx, but this was not significant. The anti-LL-37 antibody (αLL-37) significantly blocked LL-37 from binding to MSC surface receptors, as MSCs in this experimental group did not invade as effectively (Fig. 1*E*). By contrast, the anti-LL-37 antibody did not affect EGF stimulation of MSC invasion. An IgG control antibody did not interfere with the ability of LL-37 or EGF to induce MSC invasion (data not shown). Taken together, these data suggest that LL-37 induces MSC trafficking through a $G_{\alpha i}$-coupled receptor, such as FPRL1.

As further validation of FPRL1 involvement in LL-37-mediated responses, MSCs were assessed for activation of signaling molecules downstream of this receptor. Western blot analysis of MSC lysates showed that ERK-1 and -2 are robustly phosphorylated beginning 10 min after LL-37 treatment and maintained over 60 min (Fig. 1 *F* and *G*). However, MSCs pretreated with Ptx before stimulation by LL-37 reduced ERK-1/2 activation, providing further evidence in support of notion that LL-37 stimulates MSCs through FPRL1.

The growth kinetics of MSCs were then analyzed after treatment with increasing doses of recombinant LL-37 in the presence of serum. After a 72-hour time course, LL-37 failed to stimulate the proliferation of MSCs (data not shown).

Tumor-Derived LL-37 Functions as a Chemoattractant for MSCs in Vivo. To assess the importance of LL-37 in recruitment of MSCs to tumors, an in vivo migration assay was used. Human tumor xenografts were established in SCID mice by injection of OVCAR-3 ovarian cancer cells, whose expression of hCAP-18/LL-37 was previously reported (1). After 3.5 weeks, mice were randomly divided into 2 groups. One group ($n = 11$) was given an IgG control antibody and the other group ($n = 14$) was given an anti-LL-37 antibody to neutralize the peptide's effect before injection of firefly luciferase (ffLUC)-labeled MSCs. Bioluminescence images were taken throughout the experiment to monitor engraftment of MSCs into the developing ovarian tumors. Neutralization of tumor-derived LL-37 in anti-LL-37 antibody-treated animals (αLL-37) abrogated the number of engrafted MSCs into tumors compared with IgG-treated animals (Fig. 2*A*). Bioluminescence from engrafted MSCs was quantified, and a significant difference was observed between IgG-treated animals and anti-LL-37-treated animals for each day an image was taken (Fig. 2*B*).

At the end of the experiment, tumors were analyzed via immunohistochemical staining to confirm the reduced MSC engraftment into tumors of anti-LL-37-treated animals. MSCs were identified with an anti-ffLUC antibody, and their engraftment into the tumor stroma as fibroblast-like cells was readily observed (Fig. 2 *C* and *D*; white arrows). The difference in overall MSC engraftment between IgG- and anti-LL-37-treated was evident in these representative sections, validating bioluminescence imaging. In addition to ffLUC, tumor sections were co-stained for expression of LL-37. Tumor cells of IgG-treated mice expressed measurable levels of hCAP-18/LL-37, whereas expression of the peptide was dramatically reduced in tumors of anti-LL-37-treated mice (Fig. 2*C*). Surprisingly, co-localization of ffLUC and LL-37 was noted in tumor-infiltrating MSCs and, when compared with tumor cells, MSCs expressed considerably higher levels of hCAP-18/LL-37 (Fig. 2 *C* and *F*). MSCs were also noted in perivascular regions neighboring vessels, indicative of pericyte-like differentiation of these cells (Fig. 2*F*).

Neutralization of Tumor-Derived LL-37 Reduces Tumor Growth. Of the 11 tumor-bearing animals that received the IgG control antibody, 10 animals had visible tumors upon sacrifice. By contrast, 5 of the 14 animals given the anti-LL-37 antibody treatment regimen had no detectable tumor mass. Tumors from both groups were weighed after surgical removal and those from IgG-treated animals were significantly larger than those from anti-LL-37-treated animals (98.43 ± 13.51 mg vs. 46.39 ± 12.65 mg, respectively; Fig. 3*A*). To confirm these observations, tumors were stained for the proliferation marker Ki-67. A dramatic difference was again noted between tumors from IgG- and anti-LL-37-treated animals. Tumor nuclei of IgG-treated mice were almost all positive for Ki-67, in contrast to the few positive nuclei in tumors from LL-37 antibody-treated mice (Fig. 3*B*). Quantification of Ki-67$^+$ nuclei in both treatment groups revealed a statistically significant difference (Fig. 3*C*). Notably, the stromal components of tumors from anti-LL-37-treated mice, including fibroblasts and endothelial cells, were absent in a large majority of areas (Fig. 3*B*; yellow arrows). Necrotic regions were also common in tumors from anti-LL-37-treated animals, but not in IgG-treated tumors. As shown in Fig. 3*D*, these necrotic areas stained positively for LL-37, suggesting that the peptide is

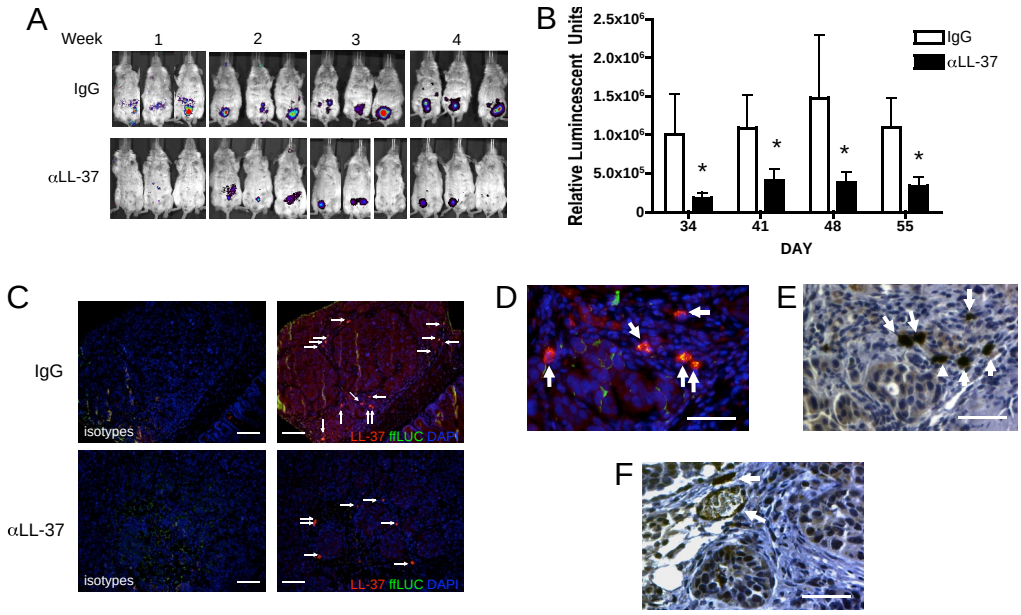

Fig. 2. Inhibition of LL-37 significantly reduces engraftment of MSCs into ovarian tumors. Human ovarian tumor xenografts were established i.p. in SCID mice. Mice were treated with IgG or anti-LL-37 antibodies (αLL-37) twice a week for 4 weeks. ffLUC-labeled MSCs were injected 4 times at weekly intervals 1 day after the first weekly injection of antibody, then visualized by bioluminescence in live mice. (*A*) Representative images of MSC engraftment into ovarian tumors 7 days after each injection of MSC. (*B*) Quantification of luminescence units emanating from tumor-engrafted MSCs. Values are mean ± SE. $*P < 0.05$. (*C*) Expression of LL-37 (red) in ovarian tumor sections of IgG- and αLL-37-treated mice. MSCs were identified using an anti-ffLUC antibody (green) and are indicated by white arrows. Nuclei were detected with DAPI. Sections are magnified ×100. (Scale bar, 100 μm.) (*D*) High-powered image (×400) of tumor section fluorescently labeled as described. (*E*) Sequential section of *D* immunohistochemically stained with anti-LL-37 antibodies followed by hematoxylin counterstain. (*F*) Example of LL-37-expressing MSCs in perivascular areas. (Scale bar, 50 μm, *D–F*.)

sequestered in the debris. Taken together, these data strongly implicate a pro-tumorigenic role for tumor-derived LL-37 through its recruitment of progenitor cell populations capable of differentiating into supportive stromal cells.

MSC Exposure to LL-37 Promotes Secretion of Angiogenic and Inflammatory Molecules. It is well established that MSCs produce many trophic factors with pro-tumorigenic functions (19, 26, 30). Evidence from the in vivo experiments described here indicated that MSCs also produce LL-37. We tested conditioned medium from several MSC donor pools growing in culture by ELISA and found that these cells readily secrete the peptide (Fig. 4*A*).

Next, we set out to determine how tumor-infiltrating MSCs would react to the LL-37-rich microenvironment of ovarian tumors. We have previously reported that LL-37 enhances the secretion of IL-1β, IL-6, IL-8, IL-10, and TNF-α from MSC while diminishing the secretion of IL-12 (p70) (26). To identify additional MSC-derived cytokines and growth factors that may be regulated by ovarian tumor-derived LL-37 and expand our previous findings, conditioned medium from various LL-37-treated MSC donor pools was analyzed by Luminex-based assays. After 48 h of LL-37 treatment, MSCs were stimulated to release significantly more of the following cytokines compared with untreated cells: IL-1 receptor antagonist, IL-6, IL-10, CCL5 (regulated upon activation, normal T cell expressed and secreted; RANTES), and VEGF (Fig. 4*B*).

Conditioned medium was also analyzed for the presence and activation of matrix metalloproteinases (MMPs) by zymography assays. Untreated MSCs secreted large amounts of the MMP-2 pro-form; no noticeable difference in expression was noted in the MMP-2 pro-form, regardless of treatment (Fig. 4*C Upper*). However, enzymatic activity of the active form of MMP-2 was increased after treatment of MSCs with LL-37, EGF, and phorbol myristate acetate (PMA; Fig. 4 *C* and *D Lower*). MMP-9 activity was undetectable after any treatment, and no expression was noted in casein gels, indicating that MSCs do not secrete measurable levels of stromelysins such as MMP-3 (data not shown).

We tested whether conditioned medium from LL-37-treated MSCs could increase endothelial cell tubule formation in vitro. Serum-starved human umbilical vein endothelial cells (HUVECs) were seeded onto growth factor-reduced Matrigel in the presence of MSC-conditioned medium. As shown in Fig. 4*E*, all 3 donor pools of LL-37-treated MSC-conditioned medium stimulated HUVECs to form tubules at a faster rate than medium from untreated MSCs. HUVECs exposed to medium from LL-37-treated MSCs began to migrate and organize into tube-like structures after only 2 hours. These data not only confirmed that LL-37-treated MSC-conditioned medium con-

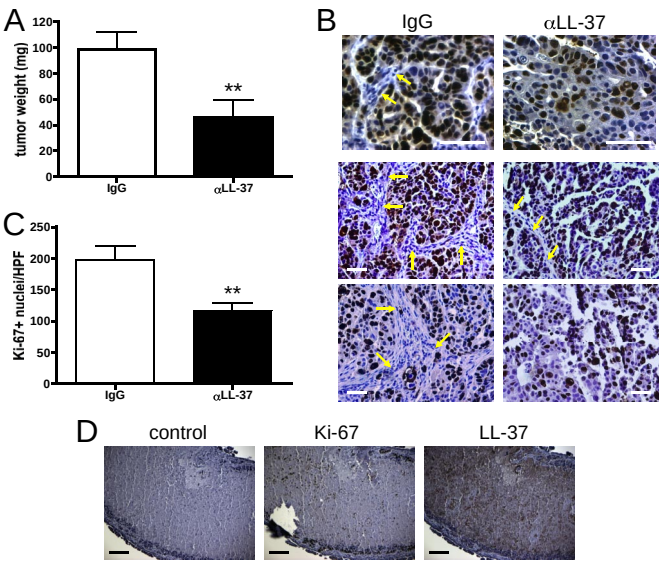

Fig. 3. Growth of ovarian tumor xenografts is diminished by neutralization of LL-37. (*A*) Graphic representation of tumor weights from IgG- ($n = 10$) and αLL-37-treated ($n = 9$) animals obtained after surgical removal. Values are mean ± SE. **, $P < 0.01$. (*B*) Representative images of tumors stained for Ki-67 with hematoxylin counterstain. Arrows indicate mouse stroma in human xenograft tumors. (Scale bar, 50 μm.) (*C*) Graphic representation of the average number of Ki-67$^+$ nuclei per high-powered field. Values are mean ± SE. **, $P < 0.01$. (*D*) Expression of Ki-67 and LL-37 in tumor necrotic region from an αLL-37-treated mouse. (Scale bar, 100 μm.)

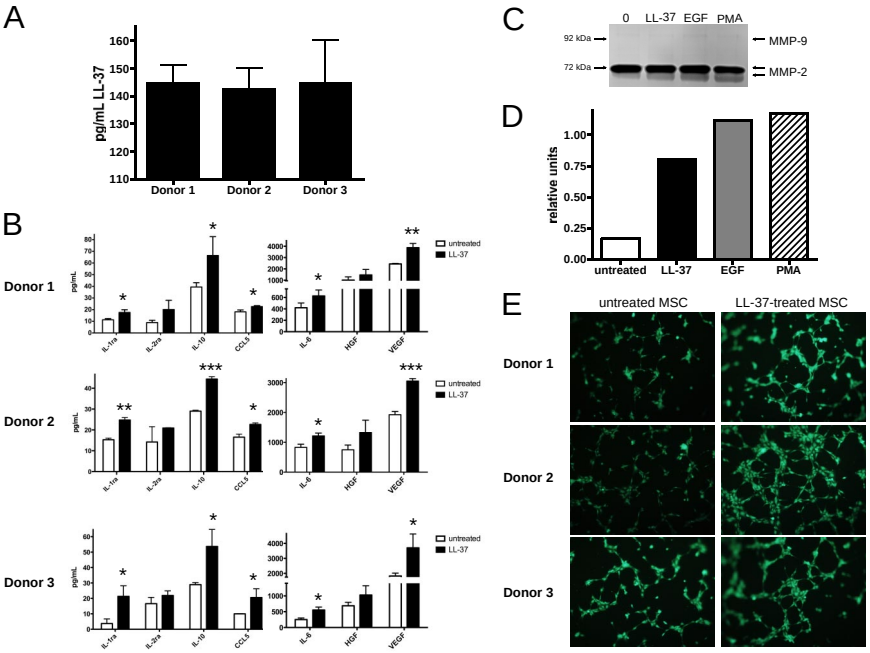

Fig. 4. MSCs secrete increased levels of angiogenic and inflammatory mediators after LL-37 stimulation. (*A*) The concentration of LL-37 in conditioned medium taken from unstimulated MSCs in culture. (*B*) Serum-starved MSCs were treated with 5 μg/mL LL-37 for 48 h, then conditioned medium was analyzed by Luminex-based cytokine arrays. Values are mean ± SE. *, $P < 0.05$, **, $P < 0.01$. (*C*) Analysis of MSC-conditioned medium after treatment for 48 h as indicated by gelatin zymography. The representative image depicts the electrophorectic pro-MMP-2 (72 kDa) and active MMP-2 (62 kDa). MMP-9 (92 kDa) was not undetectable. (*D*) Quantification of zymography by densitometry. Intensity of the lower band (active MMP-2, 62 kDa) is plotted as a bar graph ($n = 3$). (*E*) Conditioned medium from untreated and LL-37-treated MSCs was added to HUVECs, then seeded onto Matrigel. Fluorescently labeled cells were monitored were for formation of capillary-like tubules. Photographs are representative of HUVECs after 2 h incubation.

tains increased amounts of pro-angiogenic molecules, they also confirmed that the pro-angiogenic milieu is functional and has bioactivity.

LL-37 Enhances the Pro-Angiogenic Activity of MSC. Because MSCs secreted larger amounts of pro-angiogenic factors in response to LL-37, we hypothesized that tumor-associated MSCs are stimulated in the same manner by a microenvironment abundant in LL-37. To this end, serum-starved MSCs were mixed into Matrigel with and without growth factors, and then injected into the flanks of nude mice. LL-37, as well as the combination of basic FGF2 and VEGF, were added to Matrigel without cells as controls. Matrigel plugs containing growth factors, but no cells, induced a significant number of vascular channels compared with plugs without growth factors (Fig. 5 *A* and *B*). Surprisingly, the stimulation of angiogenesis by LL-37 exceeded that of the FGF2/VEGF combination at the concentrations used here. MSCs, on their own, induced a similar response as FGF2/VEGF. The numbers of vascular channels in Matrigel plugs with MSC and LL-37 were significantly greater than those containing MSCs alone or MSCs and FGF2/VEGF. However, there was no synergistic or additive effect on angiogenesis in plugs containing MSCs and growth factors, as we had anticipated. MSCs with either LL-37 or FGF2/VEGF did not significantly increase the number of vascular channels compared with plugs without cells. These data implicate dual functions for LL-37: activation of MSC as well as murine endothelial cells.

As shown in Fig. 5*C*, by using Ki-67 to identify human cells, MSCs were observed around endothelial cells, but did not incorporate into the vasculature, suggesting pericyte-like differentiation and corroborating our previous reports (18, 27). We investigated LL-37's effect on the pericyte-like differentiation of MSCs by tubule formation assay. Serum-starved MSCs were seeded onto Matrigel and treated with LL-37 or FGF2 or left untreated. LL-37 stimulated MSCs to form organized, capillary-like structures in the same manner as FGF2 treatment, whereas MSCs without growth factor influence remained as single-cell entities, indicating that LL-37 may be involved in differentiation of MSCs into pericytes in tumors (Fig. 5*D*).

Discussion

Emerging evidence indicates that inflammatory molecules play a pivotal role in tumor progression; however, the function of many of these tumor-derived inflammatory mediators remains poorly understood (31). Herein, we demonstrate that LL-37 promotes ovarian tumor progression through recruitment and engraftment of MSCs into tumors, where these cells provide pro-angiogenic and immunomodulatory factors to support tumor growth and progression.

This study directly tested the importance of a tumor-derived MSC chemotactic factor by using an in vivo assay. Previous reports from our laboratory and others suggest that additional chemokines, growth factors, and danger signals may be involved in MSC migration to tumors (17, 18, 20, 26, 27). Thus, it is unlikely that LL-37 is acting alone in the recruitment of MSCs to the tumor microenvironment given the vast production of chemotactic factors by tumor and stromal cells. In support of this notion, neutralization of LL-37 in tumor-bearing animals did not completely block MSC engraftment. Additionally, few chemokine receptors have been implicated in this process. Our recent data suggest that CCR2—the receptor for CCL2 (also called monocyte chemotactic protein 1)—is involved, as incubation of murine MSCs with anti-CCR2 blocking antibodies decreases migration of these cells (18). The data presented here indicate that LL-37 mediates MSC migration through FPRL1.

Exogenously delivered MSC incorporated into tumor stroma and maintained a fibroblast appearance or differentiated into pericyte-like cells—observations consistent with our previous reports and those of others (15–20, 23, 32–34). However, the inhibition of MSC engraftment into tumors resulted in disorganization of the fibrovascular network, strongly suggesting a critical role for LL-37 in recruitment of progenitor populations that serve as carcinoma-associated fibroblasts and pericytes. Our data suggest that MSCs, when resident in LL-37-rich tumors, are activated to release trophic factors that initiate angiogenesis and/or differentiate into blood vessel-supporting cells. Although evidence of this pro-angiogenic effect was presented here, the importance of the increased cytokine levels, such as IL-10 and CCL5, in response to LL-37 was not explored in this study. Other reports have shown that MSCs possess an innate ability to modulate the function of various immune cell

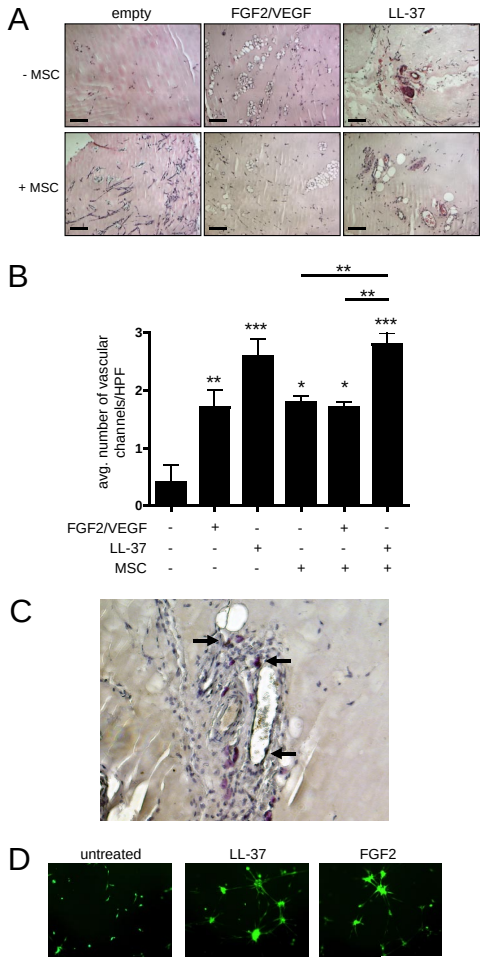

Fig. 5. LL-37 enhances the pro-angiogenic activity of MSCs. (*A*) LL-37 or the combination of FGF and VEGFA was added to cold Matrigel with or without MSCs and injected into nude mice ($n < 6$). The absence of growth factors and cells served as negative control. After 7 to 10 days, Matrigel plugs were surgically removed, fixed, sectioned, and stained by H&E. Representative images of vascular channels are shown. (Scale bar, 100 μm.) (*B*) The average number of vascular channels in each plug section was determined by counting 3 high-powered fields of view then graphically represented. Values are mean ± SE. *, $P < 0.05$, **, $P < 0.01$, ***, $P < 0.001$. (*C*) Example of MSCs in perivascular areas identified by Ki-67 staining. (*D*) Fluorescently labeled, serum-starved MSCs were seeded onto Matrigel in the presence of 5 μg/mL LL-37 or 10 ng/mL FGF2 and allowed to incubate overnight. Formation of tubules, indicative of their pericyte-like differentiation, was captured by microscopy at ×200 the next day.

populations via these factors (35, 36). Another effect of LL-37 on MSCs was the elevated secretion of CCL5. MSCs have been shown to promote breast cancer metastases through release of this cytokine, raising the possibility that LL-37 may be the instigator in this process (19).

Unexpectedly, staining for LL-37 in ovarian tumor xenograft sections proved a better identifier of MSCs than ffLUC. As noted in Fig. 2, LL-37 expression was much higher in MSCs than ovarian cancer cells, indicating that both tumor cells and MSCs contribute the peptide to the cytokine milieu of the tumor. This increase in total LL-37 levels may then lead to recruitment of more MSCs perpetuating the progression of the tumor. Perivascular MSCs may also influence endothelial cells through secretion of LL-37, as the peptide's effects on endothelial cells has already been established through FPRL1 activation (7).

The results presented here and in previous reports suggest the following sequence of events summarized in Fig. 6: (*i*) genetic

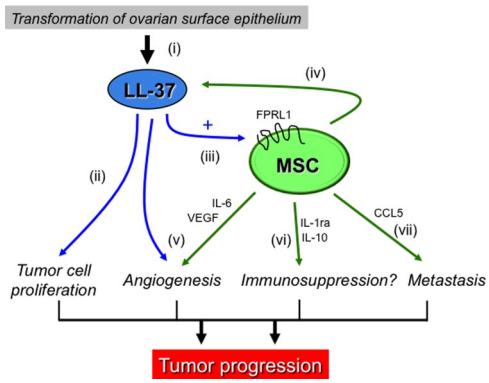

Fig. 6. Schematic illustration of effects of LL-37 and MSCs on ovarian tumor progression (see *Discussion*).

alterations in ovarian surface epithelial cells or other tissues elevates expression of LL-37, a peptide whose expression is low or absent in normal cells (1); (*ii*) LL-37 feeds back on the tumor epithelium, stimulating epithelial cell proliferation (1–3); (*iii*) LL-37 activates the MSC population to migrate into the tumor mass and enhances MSC secretion of pro-angiogenic factors; (*iv*) MSCs provide additional LL-37 to the tumor microenvironment; (*v*) LL-37 as well as other tumor- and MSC-derived molecules induce angiogenesis as the tumor expands; (*vi*) MSC produce immunosuppressive factors, likely in response to the LL-37-rich microenvironment, that function to dampen anti-tumor immunity; and (*vii*) cytokines such as CCL5 released by LL-37-stimulated MSCs enable an invasive phenotype from tumor cells. The overall consequence of LL-37's actions through its recruitment of MSCs is advancement of tumor progression.

Materials and Methods

More detailed methods are presented in *SI Materials and Methods*.

Cell Culture. Human MSC were obtained from Tulane University's Center for Gene Therapy (New Orleans, LA) and Lonza/Cambrex (Walkersville, MD). The cells were characterized by flow cytometry and various differentiation assays, and the cells were propagated as described (26, 27). MSC were used at passages no greater than 5. OVCAR-3 ovarian cancer cells were cultured as described in ref. 1.

Flow Cytometry. Anti-FPRL1 antibodies or isotype controls were detected with Alexa-488-conjugated goat anti-rabbit secondary antibodies.

Boyden Chamber Migration Assay. Chemoattractants with and without an anti-LL-37 neutralizing antibody was added to the lower compartment of a 48-well modified Boyden chamber. Serum-starved MSC were added to the upper chamber. Where indicated, MSC were pretreated with 100 ng/mL pertussis toxin (Ptx).

Invasion Assay. The assay was performed in a similar manner to migration assays using inserts coated with growth factor-reduced Matrigel.

Western Blot Analysis. LL-37-treated MSC lysates were electrophoresed and transferred to nitrocellulose membranes. Quantification of band intensity was performed using National Institutes of Health ImageJ software.

In Vivo Migration Assay. Female SCID/CB17 mice were injected i.p. with OVCAR-3 ovarian cancer cells and tumors were allowed to establish for 3.5 weeks. After this time, half the mice were treated with 50 μg of nonspecific mouse IgG antibodies or 50 μg of anti-LL-37 antibodies. Antibodies were given twice a week for the duration of the experiment. MSC were infected with 500 viral particles per cell of Ad-ffLUC-RDG, 24 h before injection. D-Luciferin was used to detect MSC, 7 d after MSC injections. Bioluminescent images were acquired from anesthetized mice with the IVIS-Xenogen system (Caliper Life Sciences, Hopkington, MA), and photons per second were measured in regions of interest using Living Image software.

Histology and IHC. Tumors were fixed in formalin solution and embedded in paraffin. Sections were stained with hematoxylin and eosin. Immunofluorescence staining for LL-37 and firefly luciferase (ff-LUC) was performed using Alexa-488- and Alexa-568-conjugated antibodies, respectively. IHC was performed as previously described using Dako's Animal Research Kit (1). Images were evaluated using a Zeiss Axioplan 2 fluorescence microscope and Intelligent Innovations software (SlideBook version 4).

Analysis of MSC-Secreted Soluble Factors. MSC-conditioned medium was analyzed by a luminex-based assay. Zymography assays were performed as before (1). Quantification of band intensity was performed using ImageJ software.

Tubule Formation Assay. HUVECs were resuspended in MSC-conditioned medium and seeded onto Matrigel then fluorescently labeled. For MSC differentiation on Matrigel, cells were treated with LL-37 or FGF2.

Matrigel Plug Assay. Female BALB/c nude mice ($n = 14$) were used as described in ref. 27. Matrigel was loaded with LL-37 (final volume = 5 μg/mL), FGF2/VEGF (final volume = 10 and 25 ng/mL, respectively), and 2.5×10^5 MSC when appropriate. Vascular channels were identified from H&E stained sections and the average number from 3 separate 400× fields was calculated for each plug.

Statistical Analyses. Student's *t* test or one-way ANOVA followed by Newman-Keuls post hoc test was used for *P* values.

ACKNOWLEDGMENTS. We thank Dr. Jeff Rosen and his team for their accommodation and Dr. Cindy Morris for the HUVECs. This work was supported in part by National Institutes of Health grants 1P20RR20152–01 (to A.B.S.) and CA-1094551, CA-116199, and CA49639 (to F.C.M.); Susan G. Komen Breast Cancer Foundation grant BCTR0504372 (to K.W., J.L.D., and F.C.M.), and the W. M. Keck Foundation.

1. Coffelt SB, et al. (2008) Ovarian cancers overexpress the antimicrobial protein hCAP-18 and its derivative LL-37 increases ovarian cancer cell proliferation and invasion. *Int J Cancer* 122:1030–1039.
2. Heilborn JD, et al. (2005) Antimicrobial protein hCAP18/LL-37 is highly expressed in breast cancer and is a putative growth factor for epithelial cells. *Int J Cancer* 114:713–719.
3. von Haussen J, et al. (2008) The host defence peptide LL-37/hCAP-18 is a growth factor for lung cancer cells. *Lung Cancer* 59:12–23.
4. Agerberth B, et al. (1995) FALL-39, a putative human peptide antibiotic, is cysteine-free and expressed in bone marrow and testis. *Proc Natl Acad Sci USA* 92:195–199.
5. Larrick JW, et al. (1995) Human CAP18: A novel antimicrobial lipopolysaccharide-binding protein. *Infect Immun* 63:1291–1297.
6. Larrick JW, Hirata M, Zhong J, Wright SC (1995) Anti-microbial activity of human CAP18 peptides. *Immunotechnology* 1:65–72.
7. Koczulla R, et al. (2003) An angiogenic role for the human peptide antibiotic LL-37/hCAP-18. *J Clin Invest* 111:1665–1672.
8. Shaykhiev R, et al. (2005) Human endogenous antibiotic LL-37 stimulates airway epithelial cell proliferation and wound closure. *Am J Physiol* 289:L842–L848.
9. Heilborn JD, et al. (2003) The cathelicidin anti-microbial peptide LL-37 is involved in re-epithelialization of human skin wounds and is lacking in chronic ulcer epithelium. *J Invest Dermatol* 120:379–389.
10. Cowland JB, Johnsen, AH, Borregaard, N (1995) hCAP-18, a cathelin/pro-bactenecin-like protein of human neutrophil specific granules. *FEBS Lett* 368:173–176.
11. Sorensen OE, et al. (2001) Human cathelicidin, hCAP-18, is processed to the antimicrobial peptide LL-37 by extracellular cleavage with proteinase 3. *Blood* 97:3951–3959.
12. Sorensen OE, et al. (2003) Processing of seminal plasma hCAP-18 to ALL-38 by gastricsin: A novel mechanism of generating antimicrobial peptides in vagina. *J Biol Chem* 278:28540–28546.
13. Yang D, et al. (2000) LL-37, the neutrophil granule- and epithelial cell-derived cathelicidin, utilizes formyl peptide receptor-like 1 (FPRL1) as a receptor to chemoattract human peripheral blood neutrophils, monocytes, and T cells. *J Exp Med* 192:1069–1074.
14. Agerberth B, et al. (2000) The human antimicrobial and chemotactic peptides LL-37 and alpha-defensins are expressed by specific lymphocyte and monocyte populations. *Blood* 96:3086–3093.
15. Studeny M, et al. (2004) Mesenchymal stem cells: Potential precursors for tumor stroma and targeted-delivery vehicles for anticancer agents. *J Natl Cancer Inst* 96:1593–1603.
16. Studeny M, et al. (2002) Bone marrow-derived mesenchymal stem cells as vehicles for intereron-beta delivery into tumors. *Cancer Res* 62:3603–3608.
17. Nakamizo A, et al. (2005) Human bone marrow-derived mesenchymal stem cells in the treatment of gliomas. *Cancer Res* 65:3307–3318.
18. Klopp AH, et al. (2007) Tumor irradiation increases the recruitment of circulating mesenchymal stem cells into the tumor microenvironment. *Cancer Res* 67:11687–11695.
19. Karnoub AE, et al. (2007) Mesenchymal stem cells within tumour stroma promote breast cancer metastasis. *Nature* 449:557–563.
20. Dwyer RM, et al. (2007) Monocyte chemotactic protein-1 secreted by primary breast tumors stimulates migration of mesenchymal stem cells. *Clin Cancer Res* 13:5020–5027.
21. Komarova S, Kawakami Y, Stoff-Khalili MA, Curiel DT, Pereboeva L (2006) Mesenchymal progenitor cells as cellular vehicles for delivery of oncolytic adenoviruses. *Mol Cancer Ther* 5:755–766.
22. Stoff-Khalili MA, et al. (2007) Mesenchymal stem cells as a vehicle for targeted delivery of CRAds to lung metastases of breast carcinoma. *Breast Cancer Res Treat* 105:157–167.
23. Khakoo AY, et al. (2006) Human mesenchymal stem cells exert potent antitumorigenic effects in a model of Kaposi's sarcoma. *J Exp Med* 203:1235–1247.
24. Ramasamy R, et al. (2007) Mesenchymal stem cells inhibit proliferation and apoptosis of tumor cells: Impact on in vivo tumor growth. *Leukemia* 21:304–310.
25. Djouad F, et al. (2003)Immunosuppressive effect of mesenchymal stem cells favors tumor growth in allogeneic animals. *Blood* 102:3837–3844.
26. Tomchuck SL, et al. (2008) Toll-like receptors on human mesenchymal stem cells drive their migration and immunomodulating responses. *Stem Cells* 26:99–107.
27. Zwezdaryk KJ, et al. (2007) Erythropoietin, a hypoxia-regulated factor, elicits a pro-angiogenic program in human mesenchymal stem cells. *Exp Hematol* 35:640–652.
28. Spaeth E, Klopp A, Dembinski J, Andreeff M, Marini F (2008) Inflammation and tumor microenvironments: Defining the migratory itinerary of mesenchymal stem cells. *Gene Ther* 15:730–738.
29. Viswanathan A, Painter RG, Lanson NA, Jr, Wang, G (2007) Functional expression of N-formyl peptide receptors in human bone marrow-derived mesenchymal stem cells. *Stem Cells* 25:1263–1269.
30. Uccelli A, Moretta, L, Pistoia, V (2008) Mesenchymal stem cells in health and disease. *Nat Rev Immunol*, in press.
31. Coffelt SB, Scandurro, AB (2008) Tumors sound the alarmin(s). *Cancer Res* 68:6482–6485.
32. Au P, Tam J, Fukumura D, Jain RK (2008) Bone marrow-derived mesenchymal stem cells facilitate engineering of long-lasting functional vasculature. *Blood* 111:4551–4558.
33. Covas DT, et al. (2008) Multipotent mesenchymal stromal cells obtained from diverse human tissues share functional properties and gene-expression profile with CD146+ perivascular cells and fibroblasts. *Exp Hematol* 36:642–654.
34. Mishra PJ, et al. (2008) Carcinoma-associated fibroblast-like differentiation of human mesenchymal stem cells. *Cancer Res* 68:4331–4339.
35. Beyth S, et al. (2005) Human mesenchymal stem cells alter antigen-presenting cell maturation and induce T-cell unresponsiveness. *Blood* 105:2214–2219.
36. Ren G, et al. (2008) Mesenchymal stem cell-mediated immunosuppression occurs via concerted action of chemokines and nitric oxide. *Cell Stem Cell* 2:141–150.
37. Yotnda P, et al. (2004) Comparison of the efficiency of transduction of leukemic cells by fiber-modified adenoviruses. *Hum Gene Ther* 15:1229–1242.

Leucine Leucine-37 Uses Formyl Peptide Receptor–Like 1 to Activate Signal Transduction Pathways, Stimulate Oncogenic Gene Expression, and Enhance the Invasiveness of Ovarian Cancer Cells

Seth B. Coffelt,[1] Suzanne L. Tomchuck,[2] Kevin J. Zwezdaryk,[2] Elizabeth S. Danka,[2] and Aline B. Scandurro[2]

[1]Tumour Targeting Group, Academic Unit of Pathology, University of Sheffield, Sheffield, United Kingdom and [2]Department of Microbiology and Immunology, Tulane University, New Orleans, Louisiana

Abstract

Emerging evidence suggests that the antimicrobial peptide, leucine leucine-37 (LL-37), could play a role in the progression of solid tumors. LL-37 is expressed as the COOH terminus of human cationic antimicrobial protein-18 (hCAP-18) in ovarian, breast, and lung cancers. Previous studies have shown that the addition of LL-37 to various cancer cell lines *in vitro* stimulates proliferation, migration, and invasion. Similarly, overexpression of hCAP-18/LL-37 *in vivo* accelerates tumor growth. However, the receptor or receptors through which these processes are mediated have not been thoroughly examined. In the present study, expression of formyl peptide receptor–like 1 (FPRL1) was confirmed on ovarian cancer cells. Proliferation assays indicated that LL-37 does not signal through a G protein–coupled receptor, such as FPRL1, to promote cancer cell growth. By contrast, FPRL1 was required for LL-37–induced invasion through Matrigel. The peptide stimulated mitogen-activated protein kinase and Janus-activated kinase/signal transducers and activators of transcription signaling cascades and led to the significant activation of several transcription factors, through both FPRL1-dependent and FPRL1-independent pathways. Likewise, expression of some LL-37–stimulated genes was attenuated by the inhibition of FPRL1. Increased expression of CXCL10, EGF, and PDGF-BB as well as other soluble factors was confirmed from conditioned medium of LL-37–treated cells. Taken together, these data suggest that LL-37 potentiates a more aggressive behavior from ovarian cancer cells through its interaction with FPRL1. (Mol Cancer Res 2009;7(6):907–15)

Received 7/10/08; revised 2/10/09; accepted 3/2/09; published OnlineFirst 6/2/09.

Grant support: NIH 1P20RR20152-01.

The costs of publication of this article were defrayed in part by the payment of page charges. This article must therefore be hereby marked *advertisement* in accordance with 18 U.S.C. Section 1734 solely to indicate this fact.

Note: Supplementary data for this article are available at Molecular Cancer Research Online (http://mcr.aacrjournals.org/).

Current address for S.B. Coffelt: Tumour Targeting Group, Academic Unit of Pathology, University of Sheffield, Sheffield, United Kingdom.

Requests for reprints: Seth B. Coffelt, Tumour Targeting Group, University of Sheffield School of Medicine, Academic Unit of Pathology, EU24, Sheffield, UK S10 2RX. Phone: 44-114-271-2733; Fax: 44-271-1711. E-mail: s.coffelt@sheffield.ac.uk

doi:10.1158/1541-7786.MCR-08-0326

Introduction

Inflammatory molecules play a pivotal role in tumorigenesis and cancer progression (1). Recently, we have shown that one specific inflammatory molecule, called leucine leucine-37 (LL-37), is highly expressed in epithelial ovarian tumors, and reports from other laboratories indicate that breast and lung tumors also express elevated levels of LL-37 (2-4). However, little is known about the mechanism of action of LL-37 on tumor cells. LL-37 is the 37–amino acid peptide derivative of human cationic antimicrobial protein-18 (hCAP-18), originally identified as a product of various leukocytes (5-7). In recent years, expression of LL-37 has also been detected in other cell types such as epithelia, in which inflammatory stimuli can up-regulate peptide expression (8). Cleavage of hCAP-18 gives rise to two functionally distinct peptides, the importance of which in host defense against microorganisms has been clearly defined (5, 6, 9). In addition to its antimicrobial functions, LL-37 also plays a role in wound healing, angiogenesis, and leukocyte trafficking (10-19). LL-37 initiates these responses through multiple receptors including the $G\alpha_i$ protein–coupled receptor (GPCR), formyl peptide receptor–like 1 (FPRL1), the epidermal growth factor receptor (EGFR), the purinergic receptor $P2_X7$, and another receptor (or receptors) that remains uncharacterized (12, 13, 15-17, 19-22). Unlike FPRL1 and $P2_X7$ activation, EGFR activation does not occur through direct interaction with LL-37. Rather, EGFR is transactivated by LL-37–induced metalloproteinase cleavage of membrane-associated EGFR ligands, and this effect may be GPCR-dependent or GPCR-independent according to cell type (12, 13, 20).

Our previous study suggested that LL-37 facilitates tumor progression through multiple mechanisms, as treatment of ovarian cancer cells with recombinant peptide resulted in increased proliferation, migration, invasion, and matrix metalloproteinase (MMP) activation (2). In agreement with these data, other laboratories have shown that LL-37 stimulates the proliferation of various cancer cell lines and that overexpression of hCAP-18/LL-37 in lung cancer xenografts increases tumor growth in nude mice (3, 4). More recently, hCAP-18/LL-37 has been shown to contribute to breast cancer metastases (23). Transactivation of EGFR and ErbB2, two members of the EGFR family, has been implicated in mediating the effects of LL-37 through the use of pharmacologic inhibitors. However, the

specific involvement of FPRL1 has not been thoroughly examined, as only a general inhibitor of $G\alpha_i$ signaling (i.e., pertussis toxin) has been used to date. Therefore, we set out to investigate the role of FPRL1 in this, and other processes, as well as the mechanism through which LL-37 influences ovarian cancer cells.

Results

A panel of seven cell lines was examined by flow cytometry for expression of FPRL1. The ovarian cancer cell lines expressed FPRL1 to varying degrees and Hs832.Tc—a fibroblastic cell line derived from a benign ovarian cyst—expressed the lowest measured levels of FPRL1 (Fig. 1). We previously reported that LL-37 induces ovarian cancer cell proliferation (2). To determine if LL-37 signals through FPRL1 to mediate this effect, the same ovarian cancer cell lines used in our prior study were pretreated with pertussis toxin (Ptx) before exposure to the LL-37 peptide. Ptx treatment reduced the proliferation rate of LL-37–treated HEY, OV-90, and SK-OV-3 cells after 48 hours; although this effect was not statistically significant (Fig. 2). These results indicate that LL-37 does not use FPRL1 (or any other $G\alpha_i$-dependent GPCR) to stimulate ovarian cancer cell growth.

Previously, we also reported that LL-37 enhances the metastatic potential of SK-OV-3 ovarian cancer cells (2). Here, we confirmed the ability of LL-37 to induce the invasive behavior of two other ovarian cancer cell lines, OV-90 and TOV-112D (Fig. 3A). LL-37–mediated chemotaxis occurs through the FPRL1 receptor in some lymphoid and myeloid subsets; therefore, we hypothesized that LL-37 uses this receptor to initiate ovarian cancer cell invasion (16, 19). To address this question, we established FPRL1 knockdown cells by transduction of SK-OV-3 cells with lentiviruses containing FPRL1-specific shRNA constructs (termed FPRL1 KD-1 to KD-5). Another shRNA construct that does not recognize a specific mRNA target (called nontargets) was used as control. *Fprl1* gene expression was measured using quantitative real-time PCR (qPCR) and it was observed that *fprl1* expression was significantly diminished in SK-OV-3/FPRL1 KD-1, KD-2, KD-3, and KD-4 cells (Fig. 3B). SK-OV-3/FPRL1 KD-2 cells were chosen for use in subsequent experiments, as the level of *fprl1* mRNA transcript was lowest in these cells. SK-OV-3 cells seeded onto Matrigel-coated inserts were then stimulated with LL-37 or EGF in an *in vitro* invasion assay. In contrast to the proliferation assay results, Ptx attenuated LL-37–induced SK-OV-3 cell invasion through Matrigel. EGF-stimulated invasion was unaffected by the inhibitor (Fig. 3C). SK-OV-3 cells transfected with control shRNA vectors (nontargets) responded to LL-37 and EGF stimulation in a similar manner as untransfected cells (Fig. 3D). EGF exposure significantly augmented the invasive behavior of SK-OV-3/FPRL1 KD-2, but LL-37 stimulation failed to significantly enhance their invasion when compared with untreated, knockdown cells. Taken together, these data suggest that LL-37 signals through FPRL1 to increase the metastatic potential of ovarian cancer cells.

To better define the signaling pathways that are activated by LL-37, several of the established FPRL1-associated and EGFR-associated signaling cascades were studied (3, 4, 10, 12, 15, 20, 24). Western blot analysis of LL-37–treated SK-OV-3 cell lysates showed the robust phosphorylation of ERK1/2 and a slight activation of signal transducers and activators of transcription (STAT) 3, after the indicated time points (Fig. 4A). By contrast, AKT activation was constitutive for the time points measured. Similar results were observed in LL-37–treated OVCAR-3 cells (data not shown). SK-OV-3 cells were

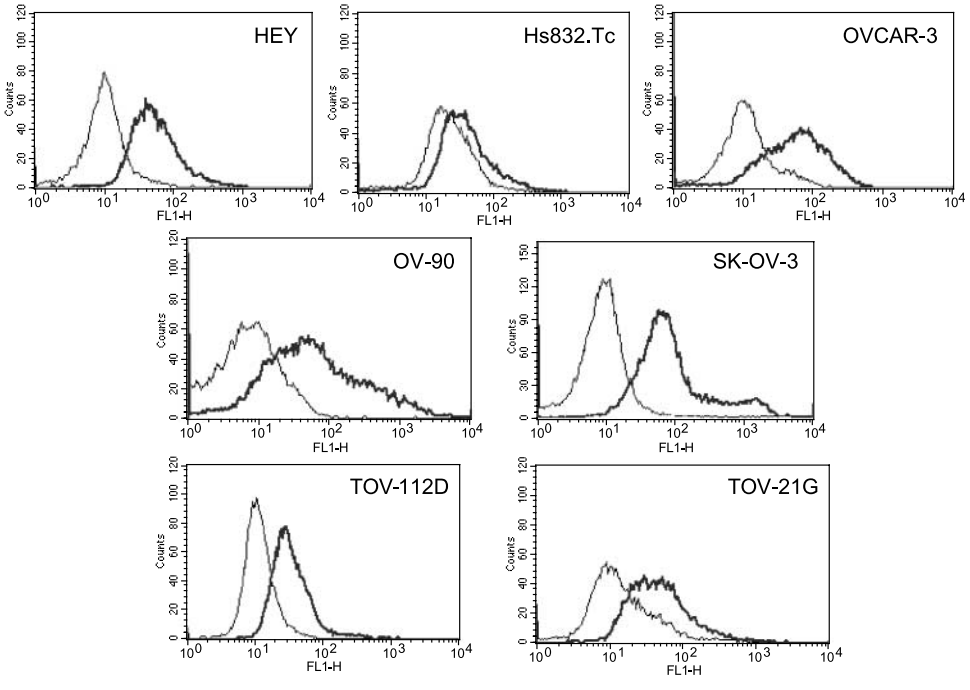

FIGURE 1. FPRL1 is expressed on ovarian cancer cells. Ovarian cancer cell lines, representing different histologic subtypes, were analyzed for FPRL1 expression by flow cytometry. Primary antibodies were detected with Alexa-488–conjugated goat anti-rabbit antibodies. Black line, FPRL1 expression; gray line, isotype control ($n = 3$).

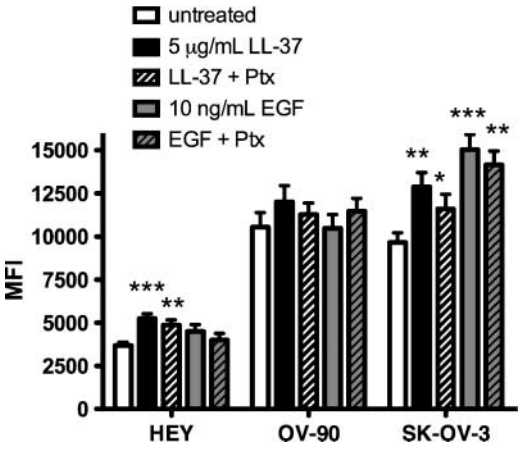

FIGURE 2. LL-37 does not signal through a GPCR, such as FPRL1, to stimulate ovarian cancer cell proliferation. Graphic representation of ovarian cancer cell growth after exposure to LL-37 or EGF. Serum-starved cells were pretreated with or without 10 ng/mL of Ptx for 1 h, followed by LL-37 or EGF treatment. After 48 h, cellular DNA was measured using fluorescent probes. MFI, mean fluorescence intensity. Columns, mean of three or more independent experiments; bars, SE.

pretreated with Ptx before LL-37 stimulation, but ERK1/2 phosphorylation was maintained despite inhibition of $G\alpha_i$/GPCR signaling (Fig. 4B). These observations were confirmed using SK-OV-3/FPRL1 KD-2 cells, indicating that LL-37–induced mitogen-activated protein kinase (MAPK) signaling does not occur through FPRL1 (or another GPCR).

Nuclear protein extracts isolated from LL-37–treated ovarian cancer cells were then analyzed using a Luminex-based assay, as a quantitative measurement of LL-37–activated signaling pathways at the transcription factor level. This method allowed us to measure not only nuclear accumulation of the transcription factors, but also activation, because fluorescence intensity is based on DNA binding activity to specific oligonucleotide probes. LL-37 induced a number of transcription factors in SK-OV-3 and OVCAR-3 cells; however, only those transcription factors that were increased more than 4-fold were analyzed for statistical significance. The transcription factors that were significantly increased in both cell lines when compared with untreated cells included cAMP-responsive element binding protein (CREB), ELK1, estrogen receptor, FAST1, GATA, glucocorticoid receptor/progesterone receptor, PPAR, PAX3, STAT4, and YY1 (Fig. 5A). In SK-OV-3 cells,

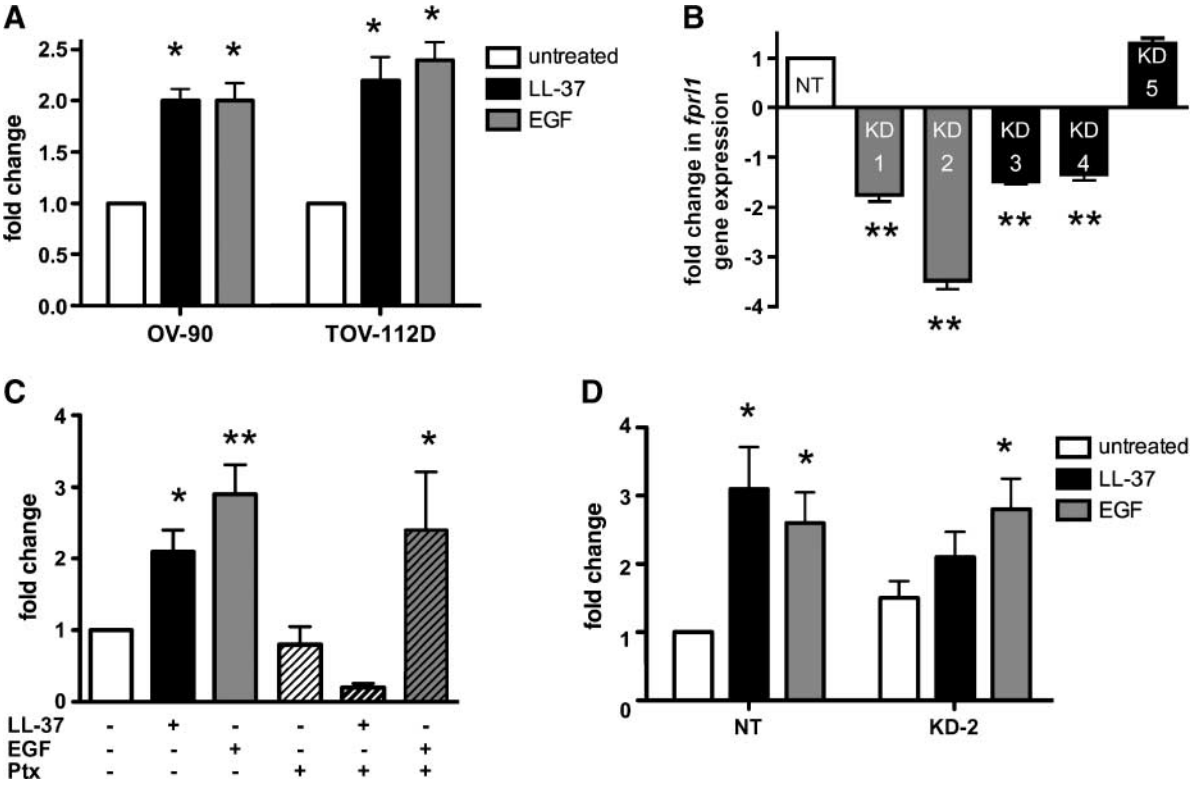

FIGURE 3. LL-37 mediates ovarian cancer cell migration and invasion through FPRL1. **A.** Graphic representation of ovarian cancer cell invasion. Serum-starved cells were seeded onto Matrigel-coated inserts in medium containing 10 μg/mL of LL-37 or 10 ng/mL of EGF. Columns, mean fold change of the mean fluorescence intensity of invaded cells compared with unstimulated controls; bars, SE ($n = 3$). **B.** Graph depicting *fprl1* gene expression in knockdown (*KD*) cells. SK-OV-3 cells stably transduced with lentiviruses containing FPRL1-specific shRNA (*KD-1* to *KD-5*) or nontarget (*NT*) sequences were analyzed by qPCR. Columns, mean of three independent experiments compared with nontarget cells; bars, SE. **C.** Graphic representation of SK-OV-3 ovarian cancer cell invasion through Matrigel-coated inserts. Untreated and Ptx-treated SK-OV-3 cells were stimulated with LL-37 or EGF as described above. *P* values for LL-37 or EGF groups were determined from their respective untreated or Ptx-treated alone controls. **D.** Graphic representation of SK-OV-3 nontarget cells and FPRL1 KD-2 cell invasion stimulated with LL-37 or EGF as above (*, $P < 0.05$; **, $P < 0.01$).

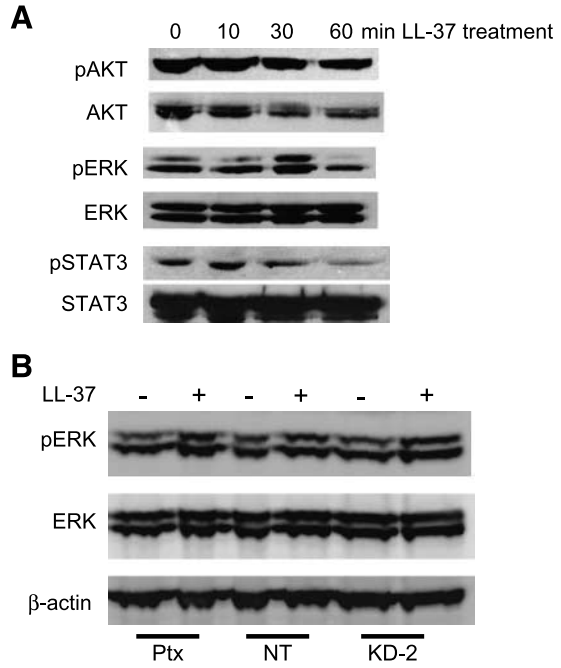

FIGURE 4. Activation of MAPK signaling pathways by LL-37 does not occur through FPRL1. **A.** The influence of recombinant LL-37 (5 μg/mL) on phosphorylation of AKT, ERK, and STAT3 in SK-OV-3 cells. Images are representative of three or more independent experiments. **B.** Cellular protein was isolated from Ptx-treated SK-OV-3 cells, SK-OV-3 nontarget cells, and SK-OV-3/FPRL1 KD-2 cells that were treated with LL-37 for 30 min. Phosphorylation and expression of ERK was measured by Western blot analysis. β-actin levels were assessed to ensure equal loading.

AP-2, ATF2, IRF, and Nkx-2.5 were also significantly induced, whereas C/EBP, Ets PEA, MyoD, and SMAD were not. LL-37 treatment of OVCAR-3 cells resulted in significant activation of HIF-1, MyoD, p53, STAT1, and STAT3, but not Ets PEA, IRF, and Nkx-2.5. The transcription factors that were not expressed in either cell line or not increased more than 4-fold by LL-37 included activator protein-1, androgen receptor, Brn3, c-myb, E2F1, FKHR, HNF1, ISRE, MEF2, NF-1, NFAT, NF-E2, NF-κB, NF-Y, Oct, PAX5, RUNX AML, and STAT5 (data not shown).

Nuclear accumulation and activity of the transcription factors significantly enhanced in both ovarian cancer cell lines were also analyzed in SK-OV-3/FPRL1 KD-1, KD-2 cells, and Ptx-treated cells after LL-37 stimulation. CREB, ELK1, estrogen receptor, GATA, and YY1 were inhibited in cells lacking FPRL1 as well as Ptx-treated cells, suggesting that LL-37 induces these transcription factors through FPRL1 signaling (Fig. 5B). For each transcription factor examined, SK-OV-3/FPRL1 KD-1 cells exhibited more activity than FPRL1 KD-2 cells, which was consistent with qPCR data indicating that SK-OV-3/FPRL1 KD-1 cells express higher levels of the FPRL1 receptor. The activity of FAST1 and glucocorticoid receptor/progesterone receptor were significantly reduced in FPRL1 KD-2 cells, but not in FPRL1 KD-1 cells or Ptx-treated cells, whereas STAT4 activity was significantly diminished only in Ptx-treated cells. These data suggest that LL-37 signals through both FPRL1-dependent and FPRL1-independent pathways.

To determine which genes are regulated by the LL-37–FPRL1 interaction in ovarian cancer cells, RNA was isolated from SK-OV-3 and OVCAR-3 cells after treatment with the peptide and analyzed by focused gene microarray. The expression profiles of 168 angiogenic and inflammatory genes were monitored after LL-37 treatment (Supplementary Table S1). Several of these genes were chosen for further validation by qPCR based on the magnitude of change in gene expression. These genes included angiopoietin-like 3 (*angptl3*), complement 5 (*c5*), collagen type XVIII (*col18a1*), epidermal growth factor (*egf*), fibroblast growth factor 1 (*fgf1*), *fprl1*, and *hcap-18/ll-37*. The matrix metalloproteinases, *mmp2, mmp9*, and *mmp14*, as well as urokinase plasminogen activator (*upa*), were also analyzed in OVCAR-3 cells because we have previously shown that LL-37 increases their expression in SK-OV-3 cells. As shown in Fig. 6A, LL-37 treatment resulted in the significant induction of the following genes in both cell lines: *c5, col18a1, egf, mmp2*, and *upa*. Gene expression of *angptl3* was significantly decreased in both cell lines. In SK-OV-3 cells, *fgf1* and *hcap-18/ll-37* expression was not affected by LL-37, whereas *fprl1* transcript was significantly more abundant. The peptide increased expression of *fgf1, fprl1, hcap-18/ll-37, mmp9*, and *mmp14* in OVCAR-3 cells; although, only the *fgf1* induction was significant.

The involvement of FPRL1 in LL-37–stimulated gene expression was then assessed in knockdown and Ptx-treated cells. Expression of *c5, col18a1, mmp2* and *upa* were significantly repressed by the absence of FPRL1 signaling (Fig. 6B). In contrast, *angptl3* expression was unaffected in SK-OV-3/FPRL1 KD cells or Ptx-treated cells. Ptx pretreatment significantly decreased *egf* expression by LL-37, but this effect was not observed in FPRL1 KD cells.

The soluble factors released from ovarian cancer cells after LL-37 treatment were analyzed by a quantitative Luminex-based assay. Both LL-37–treated SK-OV-3 and OVCAR-3 cells produced significantly more CXCL10 (IP-10), EGF, and PDGF-BB when compared with untreated cells (Fig. 7A). In addition, treatment of SK-OV-3 cells led to the increased secretion of IL-1ra, IL-9, and CCL2. Exposure of LL-37 to Ptx-treated SK-OV-3 cells, stably transfected nontarget cells, or SK-OV-3/FPRL1 KD cells significantly enhanced the release of CXCL10 and EGF when compared with untreated cells (Fig. 7B). However, LL-37 failed to stimulate PDGF-BB secretion in Ptx-treated and FPRL1 KD-2 cells. These data suggest that LL-37 uses FPRL1 for PDGF-BB release, but signals through another receptor(s) to increase CXCL10 and EGF release from ovarian cancer cells.

Discussion

Recent reports suggest an autocrine role for LL-37 in tumor cell proliferation, survival, and metastasis (1-4, 23). However, little is known about the receptors through which the promiscuous peptide, LL-37, influences these processes. Here, we present data indicating that FPRL1 is not involved in LL-37–stimulated cell growth, but is involved in promoting a more aggressive phenotype in ovarian cancer cells. We also show that the peptide uses FPRL1 to induce transcription factor activation, gene expression, and soluble factor release from ovarian cancer cells. At this time, the extent to which other receptors,

such as EGFR, ErbB2, or $P2_X7$, play a role in mediating responses to LL-37 is unclear because FPRL1 was the only receptor examined in this study.

Several lines of evidence support the notion that LL-37 stimulates a more aggressive phenotype in ovarian cancer cells. We show here, and in previous studies, that LL-37 increases ovarian cancer cell migration, invasion, and MMP secretion and conclude from the present study that this effect occurs, in part, through FPRL1 signaling (2). Our data corroborate observations from other labs, which indicate that LL-37 promotes breast cancer metastases (23). Interestingly, overexpression of hCAP-18/LL-37 in breast cancer cells implanted into severe combined immunodeficiency mice does not result in more proliferative tumors, as in the case of *in vitro* experiments and lung tumor xenografts (4, 23). These observations suggest that LL-37 may function differently in hormone-dependent malignancies (i.e., ovarian and breast) than in other hormone-independent tumor types (i.e., lung), by promoting metastasis in one and proliferation in another. In keratinocytes, LL-37 promotes protease expression and induces the expression of

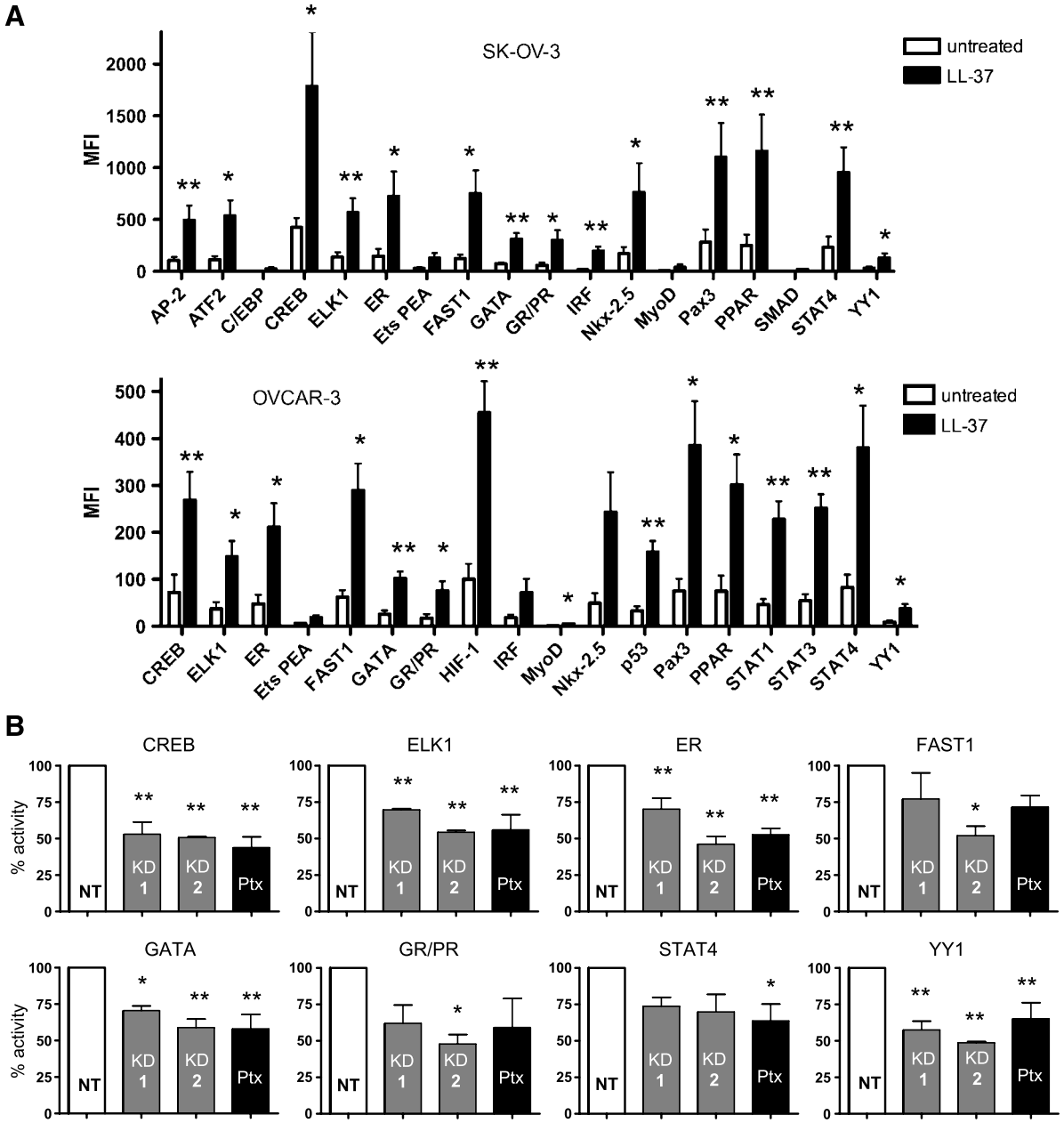

FIGURE 5. Inhibition of FPRL1 negatively affects LL-37–induced nuclear accumulation and activity of multiple transcription factors. **A.** Graphic representation of transcription factor-DNA binding. Nuclear extracts from serum-starved ovarian cancer cells, treated or untreated with 5 μg/mL of LL-37 for 1 h, were analyzed for transcription factors bound to specific fluorescently labeled oligonucleotide probes. MFI, mean fluorescence intensity. Columns, mean; bars, SE. **B.** Analysis of transcription factor activity in SK-OV-3/FPRL1 KD and Ptx-treated cells after LL-37 treatment as described above. Columns, mean of four independent experiments; bars, SE (*, $P < 0.05$; **, $P < 0.01$).

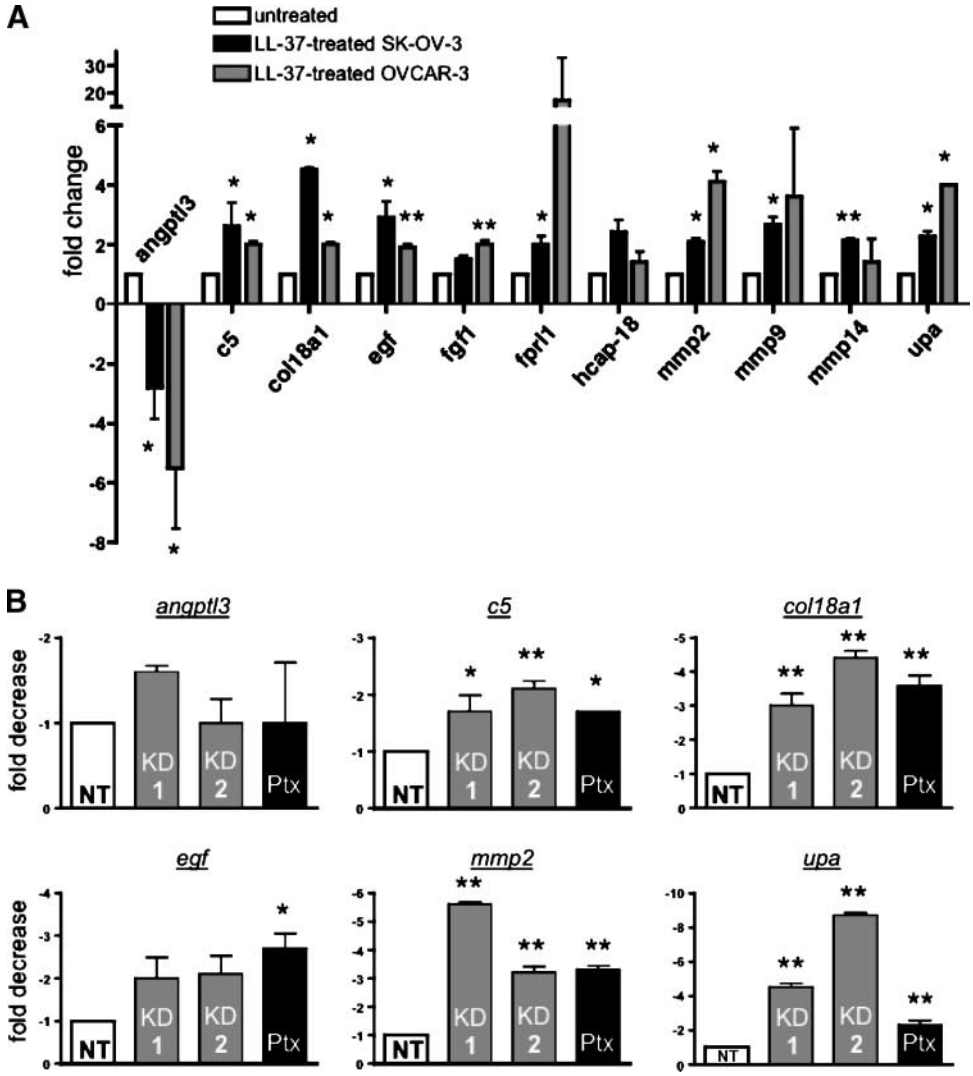

FIGURE 6. LL-37 modulates target gene expression through FPRL1 signaling. **A.** Graphic representation of genes regulated by LL-37. Serum-starved SK-OV-3 and OVCAR-3 cells were treated with 5 μg/mL of LL-37 for 6 h. RNA was isolated and analyzed by qPCR using the δCt method. **B.** Analysis of target gene expression in SK-OV-3/FPRL1 KD and Ptx-treated cells after LL-37 treatment. Columns, mean of three or more independent experiments; bars, SE (*, $P < 0.05$; **, $P < 0.01$).

molecules involved in the epithelial-to-mesenchymal transition, such as SNAIL and SLUG transcription factors (15). Thus, it is tempting to speculate that LL-37 is involved in the epithelial-to-mesenchymal transition of hormone-dependent tumors as well.

We found that LL-37 activates the MAPK signaling pathway in ovarian cancer cells and that ERK phosphorylation is maintained despite the inhibition or lack of FPRL1. This same response has now been shown for breast cancer cells, but contrasts with observations made in fibroblasts in which LL-37–induced ERK activation requires a Ptx-sensitive GPCR (23, 25). These findings highlight the promiscuous interactions of LL-37 with various receptors and indicate that its mechanism of action is cell type–specific.

A number of transcription factors were found to be downstream of LL-37–FPRL1 signaling. Activation of some of these transcription factors, such as CREB, may contribute to the invasive behavior of ovarian cancer cells by up-regulating prometastatic genes (i.e., *mmp2*), as similar findings have been shown for other cancer cell types (26). Moreover, stimulation of some transcription factors, such as STAT4, occurred in spite of the inhibition of FPRL1, whereas stimulation of others was partially abrogated in FPRL1 knockdown cells. These data suggest that not only are multiple receptors involved in LL-37 signaling, but they may also indicate that crosstalk between FPRL1 and other receptors is important for LL-37–mediated events.

LL-37 also regulated gene expression through FPRL1-dependent and FPRL1-independent pathways. Several of these genes, such as *egf, mmp2*, and *upa* have established roles in promoting tumor progression (27). The function of other genes in this process, including *angptl3, c5*, and *col18a1*, are not as well defined; although increased expression of *c5* by the LL-37–FPRL1 interaction may have important relevance to ovarian tumor progression given recently published observations in

murine tumor models (28). LL-37–induced gene expression was confirmed at the protein level for some gene products and it seemed that LL-37 regulates protein expression at the posttranslational level as well. For example, LL-37 increased EGF mRNA and protein expression, but the effect of the peptide on CXCL10 expression was seen only at the protein level because mRNA transcript levels did not change in the focused gene array analysis (Supplementary Table S1).

Taken together, these data provide further evidence in support of a protumorigenic role for LL-37 in epithelial ovarian cancers. In addition to its stimulatory effects on proliferation and the invasive behavior of ovarian cancer cells, LL-37 can also induce the release of proangiogenic factors such as EGF, PDGF-BB, and MMPs. Thus, it is likely that ovarian tumor–derived LL-37 influences both tumor epithelial cells and their microenvironment through autocrine and paracrine means—a notion supported by our recent findings indicating that LL-37 recruits progenitor cell populations to ovarian tumors (29). Although further investigations are required, the LL-37–FPRL1 interaction on tumor epithelial cells provides an attractive, potential target for cancer therapeutics.

Materials and Methods

Cell Culture

Ovarian cancer cell lines Hs832(C).T (benign ovarian cyst), OV-90 (papillary serous adenocarcinoma), SK-OV-3 (adenocarcinoma), TOV-112D (endometrioid adenocarcinoma), and TOV-21G (clear cell adenocarcinoma) were obtained from American Type Culture Collection and propagated according to their recommendations. HEY (xenograft HX-62, papillary cystadenocarcinoma) and OVCAR-3 (adenocarcinoma) cell lines were kind gifts from Frank Marini (M.D. Anderson Cancer Center, Houston, TX). These cells were maintained in RPMI 1640 (Life Technologies) containing 10% fetal bovine serum (Atlanta Biologicals) and 100 units/mL of penicillin and 100 mg/mL of streptomycin (Life Technologies).

Flow Cytometry

Ovarian cancer cells were stained with an anti–FPRL-1 antibody (1:100; LifeSpan Biosciences) or rabbit IgG isotype controls (Dako) for 30 min at 4°C after blocking in 10% goat serum. Cells were washed; then, primary antibodies were detected with Alexa-488–conjugated goat anti-rabbit secondary antibodies (1:250; Molecular Probes) for 30 min at 4°C. After washing again, analysis was done on a BD FACSCAlibur (BD Biosciences) using BD CellQuest Pro software.

Proliferation Assay

Ovarian cancer cells were seeded in 96-well plates and allowed to adhere overnight. The next day, cells were washed with PBS and serum-free medium was added. After 24 h, cells were pretreated with 10 ng/mL of Ptx for 1 h before the addition of 5 μg/mL of recombinant LL-37 (Innovagen)

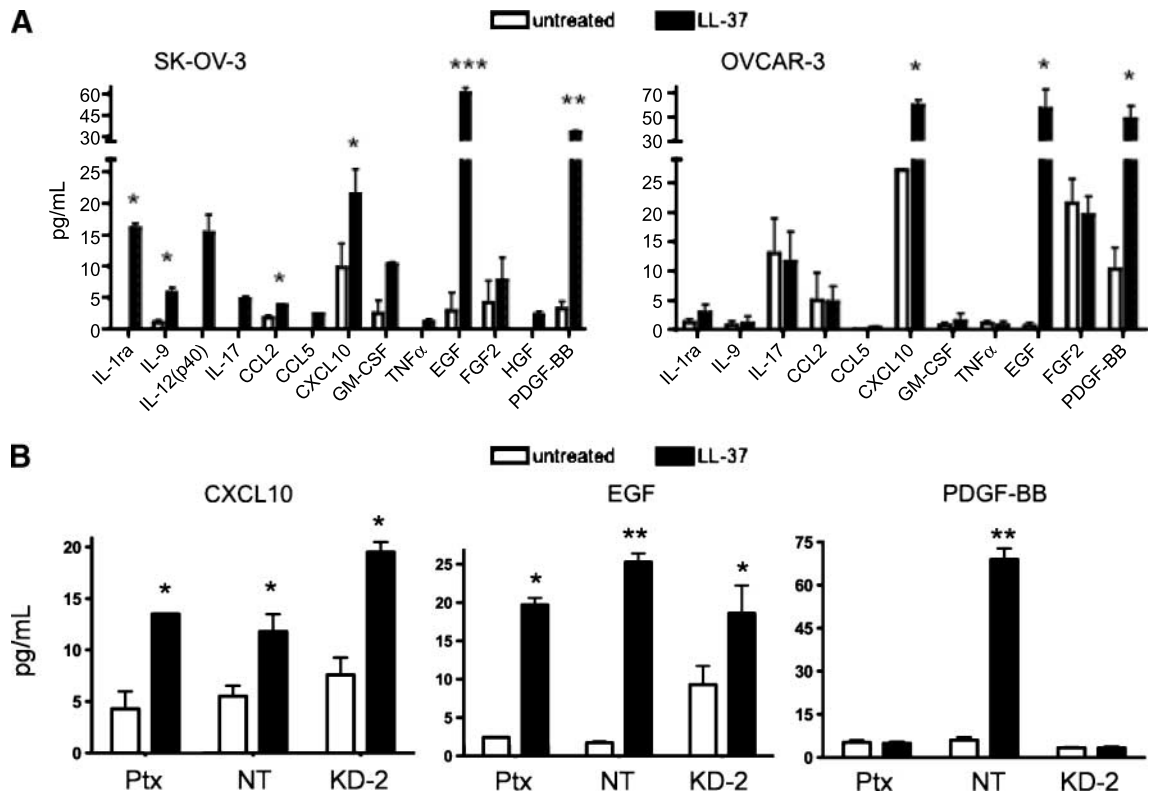

FIGURE 7. LL-37 increases the release of protumorigenic molecules from ovarian cancer cells. **A.** Serum-starved ovarian cancer cells were treated with 5 μg/mL of LL-37 for 48 h, then conditioned medium was analyzed by Luminex-based cytokine arrays. The amount of cytokines and growth factors in conditioned medium is represented graphically. **B.** Ptx-treated SK-OV-3 cells, SK-OV-3 nontarget cells, and SK-OV-3/FPRL1 KD-2 cells were treated with LL-37 as above. The levels of EGF, CXCL10, and PDGF-BB were measured in conditioned medium after 48 h. Columns, mean of three or more independent experiments; bars, SE (*, $P < 0.05$; **, $P < 0.01$; ***, $P < 0.001$).

or 10 ng/mL of EGF (R&D Systems) in medium containing 0.5% fetal bovine serum. Cells were allowed to incubate for 48 h and the remainder of the experiment was done as previously described using Invitrogen's CyQuant NF Cell Proliferation Kit (2).

Invasion Assays

Serum-starved ovarian cancer cells were assessed in invasion assays as described previously (2). Cells were pretreated with 10 ng/mL of Ptx for 1 h prior to seeding on growth factor–reduced Matrigel (BD Biosciences). LL-37 was added to a final concentration of 10 μg/mL. EGF was used at a concentration of 10 ng/mL. Both chemoattractants were added in combination with 0.5% fetal bovine serum.

Western Blot Analysis

Protein extracts were generated from LL-37–treated ovarian cancer cells, then analyzed by the same method as previously described (2, 30). All antibodies were purchased from Cell Signaling Technology and used at a concentration of 1:1,000. Horseradish peroxidase–conjugated secondary antibodies were purchased from Amersham Biosciences (1:5,000).

Transcription Factor Assay

Serum-starved ovarian cancer cells were treated with 5 μg/mL of LL-37 for 1 h. Nuclear extracts were isolated and analyzed using Panomics' Transcription Factor Assay kit following the instructions of the manufacturer on a Bio-Plex 200 (Bio-Rad).

Production of FPRL1 Knockdown Cells

SK-OV-3 cells were transduced with lentiviruses (Mission Transduction Particles; Sigma-Aldrich) containing FPRL1-specific shRNA (called KD-1 to KD-5) or nontarget sequences. Cells were treated with puromycin for 2 weeks for selection. Stable cell pools were analyzed for *fprl1* expression using real-time qPCR.

Focused Gene Array Analysis and Real-time qPCR

Total RNA was isolated from OVCAR-3 and SK-OV-3 cells following LL-37 treatment (5 μg/mL) for 6 h using the RNeasy Mini Kit (Qiagen). Purified RNA was treated with TURBO DNA-free (Ambion) before reverse transcription using SuperArray reagents or iScript (Bio-Rad) for gene array analysis or qPCR, respectively. Gene array and qPCR were done as previously described (2, 30).

Analysis of Soluble Factors Secreted by Ovarian Cancer Cells

Ovarian cancer cells were plated at a density of 1.5×10^5 in 24-well plates, allowed to adhere overnight, serum-starved for 24 h, then treated with 5 μg/mL of LL-37 in the presence of 0.5% fetal bovine serum for 48 h. Conditioned medium was collected and analyzed with Human Angiogenesis Antibody Arrays (Panomics) and Bio-Plex Cytokine Assays (Human Group I and II; Bio-Rad) on a Bio-Plex 200 (Bio-Rad) following the instructions of the manufacturer.

Statistical Analyses

Student's *t* test or one-way ANOVA followed by Newman-Keuls *post hoc* test was used to determine *P* values using GraphPad Prism software. $P < 0.05$ was considered statistically significant.

Disclosure of Potential Conflicts of Interest

No potential conflicts of interest were disclosed.

Acknowledgments

We thank Dr. Heather LaMarca for her critical review of the manuscript.

References

1. Coffelt SB, Scandurro AB. Tumors sound the alarmin(s). Cancer Res 2008;68:6482–5.

2. Coffelt SB, Waterman RS, Florez L, et al. Ovarian cancers overexpress the antimicrobial protein hCAP-18 and its derivative LL-37 increases ovarian cancer cell proliferation and invasion. Int J Cancer 2008;122:1030–9.

3. Heilborn JD, Nilsson MF, Jimenez CI, et al. Antimicrobial protein hCAP18/LL-37 is highly expressed in breast cancer and is a putative growth factor for epithelial cells. Int J Cancer 2005;114:713–9.

4. von Haussen J, Koczulla R, Shaykhiev R, et al. The host defence peptide LL-37/hCAP-18 is a growth factor for lung cancer cells. Lung Cancer 2008;59:12–23.

5. Agerberth B, Gunne H, Odeberg J, et al. FALL-39, a putative human peptide antibiotic, is cysteine-free and expressed in bone marrow and testis. Proc Natl Acad Sci U S A 1995;92:195–9.

6. Larrick JW, Hirata M, Balint RF, et al. Human CAP18: a novel antimicrobial lipopolysaccharide-binding protein. Infect Immun 1995;63:1291–7.

7. Cowland JB, Johnsen AH, Borregaard N. hCAP-18, a cathelin/pro-bactenecin-like protein of human neutrophil specific granules. FEBS Lett 1995;368:173–6.

8. Frohm M, Agerberth B, Ahangari G, et al. The expression of the gene coding for the antibacterial peptide LL-37 is induced in human keratinocytes during inflammatory disorders. J Biol Chem 1997;272:15258–63.

9. Zaiou M, Nizet V, Gallo RL. Antimicrobial and protease inhibitory functions of the human cathelicidin (hCAP18/LL-37) prosequence. J Invest Dermatol 2003;120:810–6.

10. Koczulla R, von Degenfeld G, Kupatt C, et al. An angiogenic role for the human peptide antibiotic LL-37/hCAP-18. J Clin Invest 2003;111:1665–72.

11. Heilborn JD, Nilsson MF, Kratz G, et al. The cathelicidin anti-microbial peptide LL-37 is involved in re-epithelialization of human skin wounds and is lacking in chronic ulcer epithelium. J Invest Dermatol 2003;120:379–89.

12. Tokumaru S, Sayama K, Shirakata Y, et al. Induction of keratinocyte migration via transactivation of the epidermal growth factor receptor by the antimicrobial peptide LL-37. J Immunol 2005;175:4662–8.

13. Shaykhiev R, Beisswenger C, Kandler K, et al. Human endogenous antibiotic LL-37 stimulates airway epithelial cell proliferation and wound closure. Am J Physiol Lung Cell Mol Physiol 2005;289:L842–8.

14. Jacobsen F, Mittler D, Hirsch T, et al. Transient cutaneous adenoviral gene therapy with human host defense peptide hCAP-18/LL-37 is effective for the treatment of burn wound infections. Gene Ther 2005;12:1494–502.

15. Carretero M, Escamez MJ, Garcia M, et al. *In vitro* and *in vivo* wound healing-promoting activities of human cathelicidin LL-37. J Invest Dermatol 2008;128:223–36.

16. Yang D, Chen Q, Schmidt AP, et al. LL-37, the neutrophil granule- and epithelial cell-derived cathelicidin, utilizes formyl peptide receptor-like 1 (FPRL1) as a receptor to chemoattract human peripheral blood neutrophils, monocytes, and T cells. J Exp Med 2000;192:1069–74.

17. Niyonsaba F, Iwabuchi K, Someya A, et al. A cathelicidin family of human antibacterial peptide LL-37 induces mast cell chemotaxis. Immunology 2002;106:20–6.

18. Agerberth B, Charo J, Werr J, et al. The human antimicrobial and chemotactic peptides LL-37 and α-defensins are expressed by specific lymphocyte and monocyte populations. Blood 2000;96:3086–93.

19. Tjabringa GS, Ninaber DK, Drijfhout JW, Rabe KF, Hiemstra PS. Human cathelicidin LL-37 is a chemoattractant for eosinophils and neutrophils that acts via formyl-peptide receptors. Int Arch Allergy Immunol 2006;140:103–12.

20. Tjabringa GS, Aarbiou J, Ninaber DK, et al. The antimicrobial peptide LL-37 activates innate immunity at the airway epithelial surface by transactivation of the epidermal growth factor receptor. J Immunol 2003;171:6690–6.

21. Elssner A, Duncan M, Gavrilin M, Wewers MD. A novel P2X7 receptor

activator, the human cathelicidin-derived peptide LL37, induces IL-1 β processing and release. J Immunol 2004;172:4987–94.

22. Lau YE, Rozek A, Scott MG, et al. Interaction and cellular localization of the human host defense peptide LL-37 with lung epithelial cells. Infect Immun 2005; 73:583–91.

23. Weber G, Chamorro CI, Granath F, et al. Human antimicrobial protein hCAP18/LL-37 promotes a metastatic phenotype in breast cancer. Breast Cancer Res 2009;11:R6.

24. Bowdish DM, Davidson DJ, Speert DP, Hancock RE. The human cationic peptide LL-37 induces activation of the extracellular signal-regulated kinase and p38 kinase pathways in primary human monocytes. J Immunol 2004;172:3758–65.

25. Iaccio A, Cattaneo F, Mauro M, Ammendola R. FPRL1-mediated induction of superoxide in LL-37-stimulated IMR90 human fibroblast. Arch Biochem Biophys 2009;481:94–100.

26. Melnikova VO, Mourad-Zeidan AA, Lev DC, Bar-Eli M. Platelet-activating factor mediates MMP-2 expression and activation via phosphorylation of cAMP-response element-binding protein and contributes to melanoma metastasis. J Biol Chem 2006;281:2911–22.

27. Bjorklund M, Koivunen E. Gelatinase-mediated migration and invasion of cancer cells. Biochim Biophys Acta 2005;1755:37–69.

28. Markiewski MM, DeAngelis RA, Benencia F, et al. Modulation of the antitumor immune response by complement. Nat Immunol 2008;9:1225–35.

29. Coffelt SB, Marini FC, Watson K, et al. The pro-inflammatory peptide LL-37 promotes ovarian tumor progression through recruitment of multipotent mesenchymal stromal cells. Proc Natl Acad Sci U S A 2009;106:3806–11.

30. Tomchuck SL, Zwezdaryk KJ, Coffelt SB, et al. Toll-like receptors on human mesenchymal stem cells drive their migration and immunomodulating responses. Stem Cells 2008;26:99–107.